Chem

CellPress

Article

''Dial Up and Lock In'': Asymmetric Organo-Brønsted Acid Catalysis Incorporating Stable Isotopes

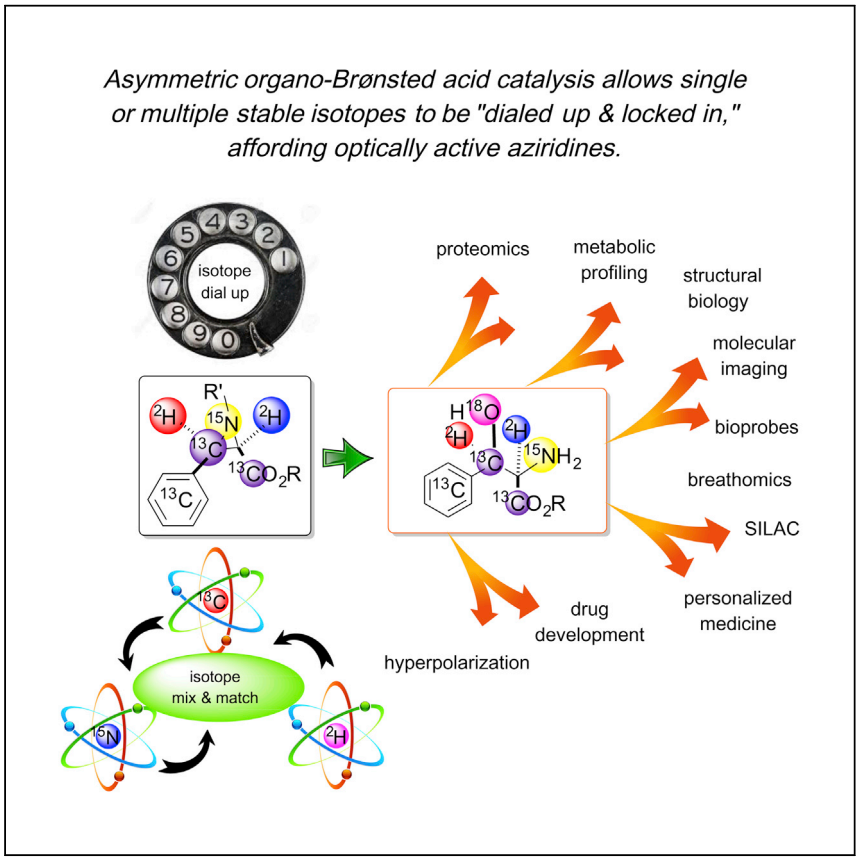

Bew and co-workers report an asymmetric organo-Brønsted-acid-catalyzed reaction that incorporates one or more stable isotopes and affords structurally and functionally diverse chiral non-racemic aziridines with excellent levels of isotope incorporation. The utility of the methodology is further substantiated by their straightforward transformation into high-value isotope-derived optically active natural and un-natural α-amino acids. The iso-organocatalysis approach advanced in this work is extendable to other reactions and should therefore prove a versatile approach to sought-after isotope-labeled compounds.

Sean P. Bew, Dominika U. Bachera, Simon J. Coles, ..., Mateusz Pitak, Sean M. Thurston, Victor Zdorichenko

s.bew@uea.ac.uk

HIGHLIGHTS

Stable-isotope incorporation mediated by organo-Brønsted acid

Asymmetric synthesis of aziridines with stable isotopes

Incorporation of single or multiple and similar or different isotopes

Generation of optically active stable-isotope-derived amino acids

Bew et al., Chem *1*, 921–945
December 8, 2016 © 2016 The Authors.
Published by Elsevier Inc.
http://dx.doi.org/10.1016/j.chempr.2016.11.008

Chem

CellPress

Article

"Dial Up and Lock In": Asymmetric Organo-Brønsted Acid Catalysis Incorporating Stable Isotopes

Sean P. Bew,[1,3,*] Dominika U. Bachera,[1] Simon J. Coles,[2] Glyn D. Hiatt-Gipson,[1] Paolo Pesce,[1] Mateusz Pitak,[2] Sean M. Thurston,[1] and Victor Zdorichenko[1]

SUMMARY

An operationally simple organo-Brønsted-acid-catalyzed asymmetric and regioselective "dial up and lock in" of one or more stable isotopes into organic compounds is unknown. Here, we describe a newly designed, chemically versatile protocol mediating single- or multiple-isotope incorporation into aziridines via a one-pot, three-component, two-step process. By exploiting easy-to-generate isotope-derived starting materials, it allows complete control of isotope positioning, affords >95 atom % isotope incorporation, and generates *cis*-aziridines with excellent optical activities and regioselectivities. Demonstrating a "low entry point," and thus easy access to a broad range of researchers, it requires no specialist laboratory equipment and employs readily attainable reaction conditions. Demonstrating their utility, the aziridines are easily transformed into sought-after chiral non-racemic α-amino acids appended with one to three (or more) identical or different isotopes. The widespread use of these compounds ensures that our methodology will be of interest to biological, medicinal, pharmaceutical, agrochemical, biotechnology, materials, and process chemists alike.

INTRODUCTION

Stable isotopes such as deuterium ([2H]), carbon ([13C]), nitrogen ([15N]), and oxygen ([18O]) are widely employed in contemporary science. Generating an isotopologue by incorporating a single isotope can propel a compound to "front line" applications in medicinal chemistry,[1] toxicology,[2] biology,[3] structural biology,[4] and mechanism determination.[5]

Differences in physical properties are evident in comparisons of otherwise identical, natural-isotope-abundant compounds with isotope-enriched isotopologues. Thus, the seemingly trivial substitution of a hydrogen atom for a deuterium atom (2-fold greater mass) affords a compound with a shorter, stronger C-[2H] bond and modifies its polarity, molar volume, Van der Waal properties, dipole moment, p*K*a, and lipophilicity; all of these can, but not always will, afford detectable chemical-reactivity and/or physicochemical differences. Isotope-dependent technologies require not only state-of-the-art instrumentation but also, importantly, convenient and efficient synthetic routes to compounds with unambiguous, site-specific isotope incorporation. Taking these points into consideration, isotope chemistry goes beyond academic interest or research curiosity; it is instead at the forefront of a raft of technologies that exploit labeled compounds in a plethora of cutting-edge applications. For example, over 3,400 volatile organic compounds (VOCs) have been

The Bigger Picture

Single- and multiple-labeled stable-isotope-derived compounds have a myriad of cutting-edge applications that span 21st century science, e.g., the development of new pharmaceuticals, the determination of protein structure, and the production of novel materials—the list goes on. Readily accessible methods that afford compounds labeled with single or multiple and identical or different isotopes are very important. Remarkably, despite global interest in organo-Brønsted acid catalysis and isotope chemistry, these have yet to be "dovetailed." We report a "one size fits all" asymmetric synthesis protocol that allows one, two, three, etc., readily available isotope-derived starting materials to be incorporated into an important class of heterocycles that are easily transformed into α-amino acids. Iso-organocatalysis affords straightforward access to labeled compounds whose long-term ubiquitous use in solving problems in academic, biological, medicinal, pharmaceutical, agrochemical, materials, and pharmaceutical sectors is, now, an easier proposition.

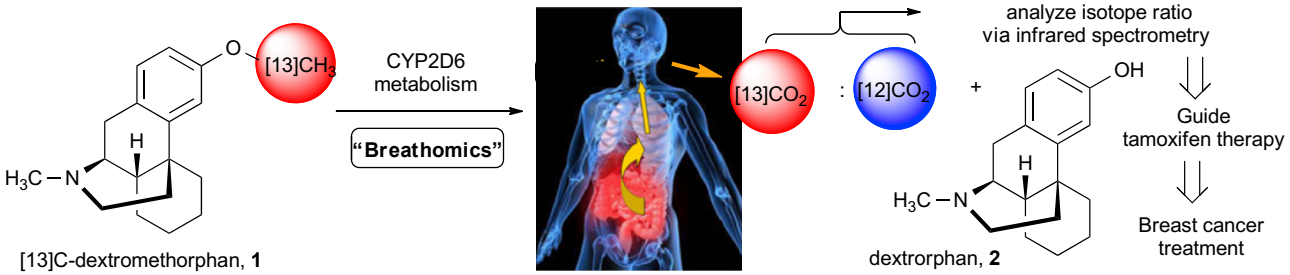

Figure 1. [13C]-Dextromethorphan 1 as a Non-invasive Breathomics Bioprobe for Breast Cancer Diagnosis

detected in deep alveolar breath.[6] This biological medium is a treasure trove of information relating to dysfunctional metabolic processes. Uniting isotope chemistry and synthetic chemistry, non-invasive "breathomics" allows a personalized-medicine approach to identifying patients who would benefit from a particular targeted therapy. The CYP2D6 metabolism of mono-[13C]-labeled dextromethorphan (**1**) is a breathomics biomarker that generates $[13C]O_2$ and **2**, as shown in Figure 1. If we compare the isotope ratios in the exhaled $[13C]O_2/[12C]O_2$ via infrared (IR) spectrometry, [13C]-**1** is a point-of-care phenotypic screen for breast cancer that can identify patients who would benefit from tamoxifen therapy.[7] Only by dovetailing the site-specific synthesis of $[13C]H_3$-**1** with an understanding of tumor metabolism and IR spectrometry is it possible to use **1** as a non-invasive precision-medicine tool. Indeed, the direct relationship among advances in state-of-the-art equipment, development of contemporary analytical techniques, and software has allowed huge gains in the detection sensitivity of isotopes. The result? An upsurge of technologies and associated synthesis methodology exploiting single- or multi-isotope-derived compounds.

The growing demand for molecules that incorporate single or multiple different isotopes can be further highlighted by their key use in biophysical analytical techniques. These include ^{1}H-NMR for in situ metabolic analysis[8] using $[13]C_2$-dopamine, in vivo screening of inhibitors using long-lifetime hyperpolarizable [13]C-[2]H-bioprobes,[9] NMR-based stereo-array [13]C-[2]H-isotope labeling for determining protein structure,[10] rate-constant analysis in enzyme-catalyzed reactions,[11] stimulated Raman scattering for imaging proteome degradation,[12] metabolic fingerprinting,[13] in vivo labeling of proteins in living cells,[14] coherent anti-Stokes Raman spectroscopy for determining the bacteriorhodpsin photocycle,[15] [13]C=[18]O-labeled peptides and 2D IR spectroscopy for amylin-inhibitor complexation,[16] stimulated emission depletion microscopy with [13]C-[15]N-α-amino acids in correlated optical and isotopic nanoscopy,[17] multi-isotope imaging mass spectrometry[18] for protein study, proteomics- and mass-spectrometry-based MARQUIS and iTRAQ using labeled peptides,[19] triple-resonance isotope-edited NMR using [13]C-[15]N-pyrimidines for monitoring catabolism and drug activity,[20] deuterated starting materials in physical organic chemistry as kinetic isotope probes of reaction mechanisms,[21] and stable-isotope-labeled pharmaceuticals as internal standards for pharmaceutical bioanalysis.[22]

Installing an isotope at a specific location within a desirable and tractable compound is an expensive, often deceptively difficult undertaking in comparison to generating its naturally abundant counterpart; the difficulty increases substantially when multiple and different isotopes are required at specific sites via a single asymmetric reaction. Catalysis underpins modern synthetic chemistry[23,24] and is built on three pillars: (1) transition-metal catalysis,[25] (2) biocatalysis,[26,27] which also includes microalgae,

[1]School of Chemistry, University of East Anglia, Norwich Research Park, Norwich, Norfolk NR4 7TJ, UK

[2]Engineering and Physical Sciences Research Council National Crystallography Service, School of Chemistry, University of Southampton, Hampshire, Southampton SO17 1BJ, UK

[3]Lead Contact

*Correspondence: s.bew@uea.ac.uk

http://dx.doi.org/10.1016/j.chempr.2016.11.008

and (3) organocatalysis; these three examples have been used exclusively to generate optically active isotope-labeled compounds. In stark contrast, the development and application of organo-Brønsted-acid-mediated protocols that transform isotope-derived starting materials into high-value products is non-existent. The third pillar must be strengthened!

Exploiting "better, milder, faster, cheaper" organocatalysis has matured to such an extent that it is now, more often than not, the first port of call in planning a synthetic route to a high-value product with a specific form and function.[28–32] Surprisingly, given all the aforementioned examples of isotope applications, two aspects of important contemporary science, that is, organo-Brønsted acid catalysis and isotope chemistry, have yet to be dovetailed together.

From an organocatalysis point of view, developing an isotope-incorporating protocol that generates compounds with one isotope or, especially, multiple and different isotopes presents specific problems that necessitate special consideration. From a reaction-screening and product-optimization perspective, both enantiomeric forms of the desired organocatalyst should be commercially available and in sufficient quantity or synthesized from cheap, readily available starting materials. To ensure widespread utilization, the starting materials should have >90% isotope enrichment. It is, however, worth noting that there are far fewer commercial-isotope-enhanced starting materials than natural-isotope-abundant starting materials. These need to be readily generated from the corresponding natural-isotope-abundant precursors with the use of commercial, easy-to-handle sources of isotope-derived reagents, e.g., [2H] → $[2H]_2O$ (e.g., Aldrich catalog no. 151882), [15N] → $[15N]H_3$ (e.g., Aldrich catalog no. 488011), [13C] → α-[13C]-benzoic acid (e.g., Aldrich catalog no. 277746), and [18O] → $H_2[18O]$ (e.g., Aldrich catalog no. 329878).

A particular concern with isotope-derived compounds or methodology incorporating isotopes is "scrambling." Yet to be developed is an organo-Brønsted acid protocol that has excellent substrate scope and allows, at will, isotope "switching"—that is, the incorporation and transformation of starting materials with multiple different or identical isotope "patterns" into isotope-defined products without scrambling and with excellent levels of incorporation. The importance of being able to "dial up and lock in"—that is, insert an isotope into a predetermined position on a molecule and ensure that it remains in position—stems from the extremely difficult task of separating scrambled compounds. Therefore, it is critical, at the outset, that a reaction be sufficiently robust that it transforms structurally and functionally diverse derived starting materials consistently and reliably into products with >95 atom % site-specific "dialed up and locked in" isotopes.

Syntheses of isotope-labeled aziridines have focused mainly on incorporating [2H] and, to a significantly lesser extent, [13C]. In summary, they utilize one or more of the following: multi-step protocols; strongly basic reaction conditions; and/or formation of hazardous nitrene intermediates that require toxic metal salts that afford, in some cases, [2H]-aziridines in low yields and/or with reduced levels of [2H] incorporation.[33–49]

As outlined in Figure 2, we report an organocatalysis milestone: a one-pot, multicomponent, asymmetric organo-Brønsted-acid-catalyzed aza-Darzens reaction that "dials up and locks in" one or more identical or different isotopes into optically active aziridines.

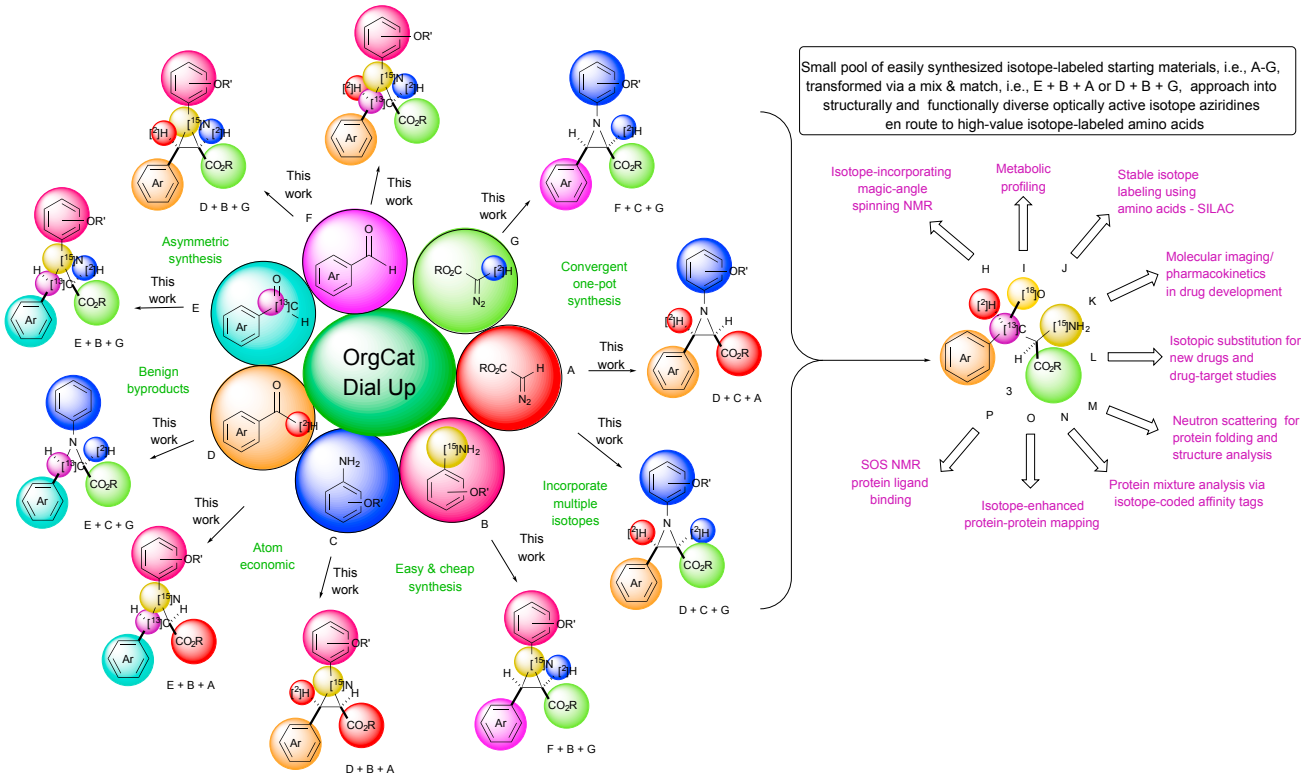

Figure 2. Isotope-Incorporating Asymmetric Organo-Brønsted Acid Catalysis

In an identical protocol, a core group of isotopologue starting materials (A–G) and a single organo-Brønsted acid afford the "dial up and lock in" (D + B + A), etc., synthesis of isotope-derived optically active aziridines. These key building blocks are easily transformed into α-amino acids with cutting-edge biotechnology-based analytical applications (H–P).

Our protocol uses an easy-to-synthesize catalyst that transforms cheap, readily synthesized starting materials into high-value aziridines with excellent levels of isotope incorporation, yield, and diastereo- and stereoselectivities. Confirming their status and utility, aziridines are readily transformed into a plethora of functionalized and optically active "secondary" products with ring opening, affording a straightforward entry point to isotope-derived natural or unnatural α-amino acids, e.g., **3** (Figure 2). Further substantiating their importance as secondary products is their transformation into sought-after tertiary products, e.g., alkaloids, antibiotics, heteroaromatic rings, and heterocyclic peptides with, again, chemoselectively "dialed in" isotopes.[50] Because non-isotope-enhanced aziridines and α-amino acids are important, it is not surprising that this extends to their isotopologue counterparts. By way of example, Figures 1 and 2 outlines select examples of cutting-edge applications for isotope-enhanced optically active α-amino acids (e.g., **3**) in a wealth of biophysical technologies, e.g., Figures 2H,[51–54] 2I,[55–57] 2J,[58–60] 2K,[61] 2L,[62,63] 2M,[64–66] 2N,[67–69] 2O,[70,71] and 2P.[72]

We report an organocatalytic approach to isotope incorporation that supplements and is complementary to transition-metal and biocatalysis approaches. A conceptually straightforward "mix and match" approach, outlined in Figure 3, includes a convenient entry point to optically active aziridines adorned with different types and numbers of identical or different isotopes and, importantly, generates them by using a handful of readily synthesized simple core starting materials. Developing an isotope-enhanced protocol should, in many respects, mirror the advantages

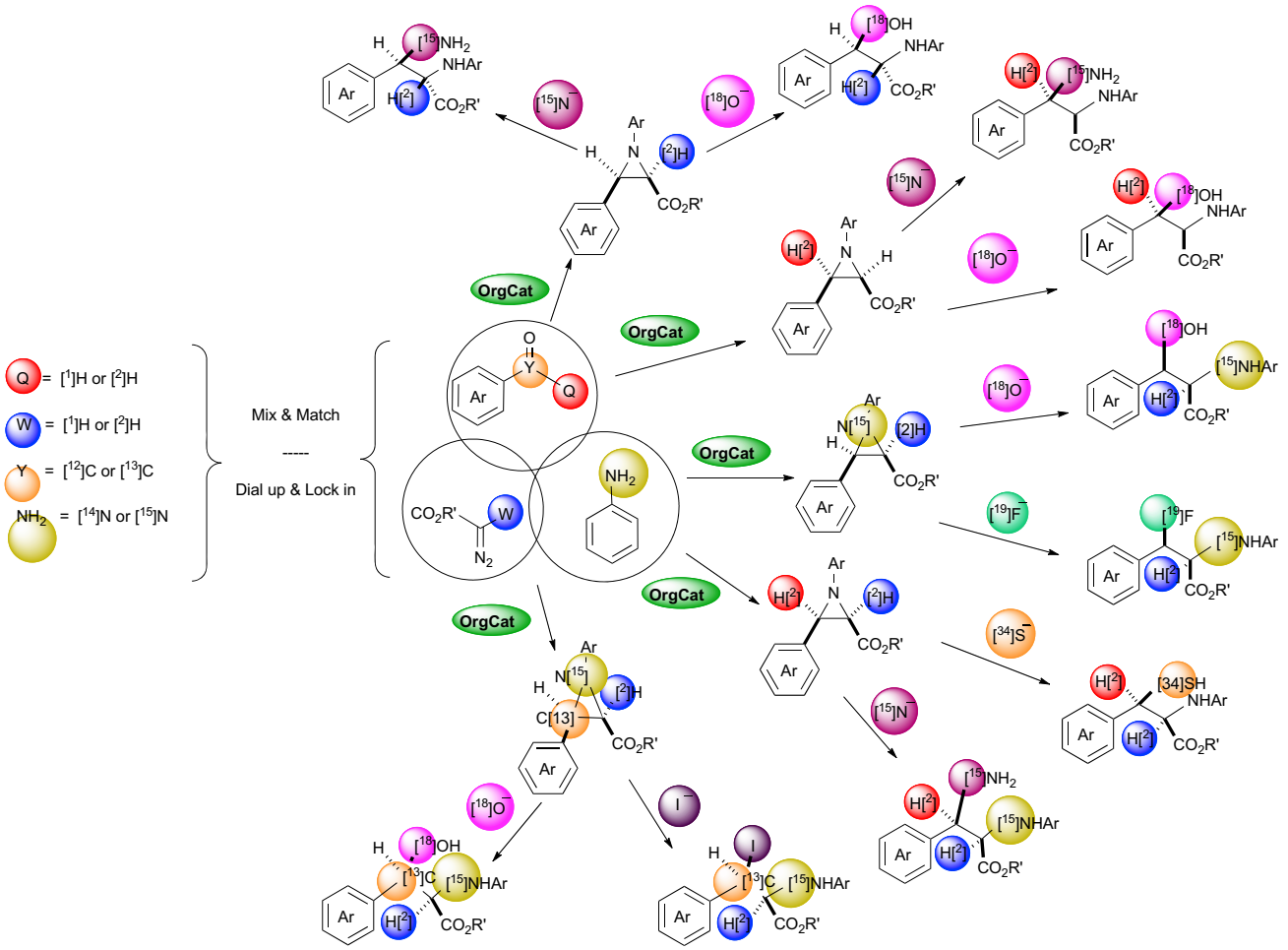

Figure 3. "Mix and Match" Approach Using a Small "Core" of Isotope-Labeled Starting Materials

A single catalyst affords a simple solution to optically active β-substituted- or α-amino acids with identical or different isotopes. Increasing numbers of divergent stable isotopes are readily incorporated, affording increasingly complex combinations of isotope-derived α-amino acids.

associated with conventional, non-isotope-enhanced organocatalytic reactions. They should be straightforward to set up, require minimal maintenance, and have no requirements for specialist equipment, e.g., gloveboxes, (photo)bioreactors, fermenters, or pressurized facilities for handling gases. Preferably, there should be no requirement for highly inert, rigorously anhydrous atmospheres or ultra-dry solvents.

Our procedure employs low-cost, "out of the box" screw-capped vials or crimp-sealed microwave tubes, and importantly, the levels of laboratory expertise required for executing single- and multi-isotope organo-Brønsted-acid-catalyzed reactions are comparable. Indeed, the process of generating one, two, three, or four, etc., isotope-derived optically active aziridines is identical. In a comparison of organic and transition-metal catalysts, the differences are clear: many of the latter require ligand and metal pre-complexation *before* the starting materials are added (often, the metal salts and/or ligands are expensive and sensitive to air and/or moisture, which complicates handling). In contrast, shelf-stable organo-Brønsted acids are weighed with no special precautions to preclude air or water; the catalyst is added with the reactants and removed by a simple filtration through alumina or silica gel. Additionally, many structurally and functionally diverse asymmetric

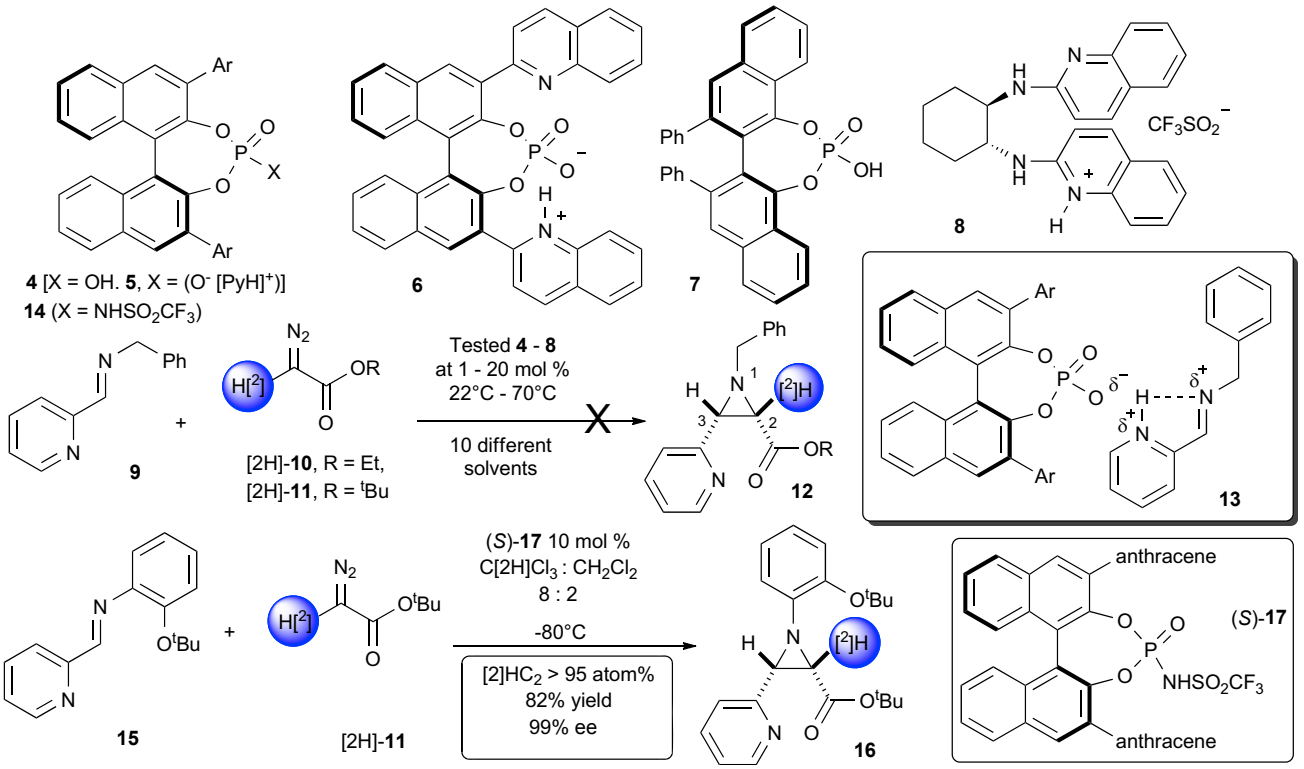

Figure 4. Failed Aziridinations Using 9–11 and BINOL-Derived Organo-Brønsted Acids 4–8
Successful asymmetric synthesis of deuterium-labeled aziridine [2H]C_2-**16** with BINOL-derived *N*-triflylphosphoramide (*S*)-**17**.

organo-Brønsted acids are commercially available in both optical forms or can be easily generated in gram quantities.

RESULTS AND DISCUSSION

Independently, both organo-Brønsted acid catalysis and multicomponent reactions[73] have an impressive and established track record of synthetic transformations. Not surprisingly, when these are dovetailed, the resulting protocols are robust and powerful methods for the construction of molecular species[74,75] augmented with complexity, but importantly, they are generated via fewer synthetic operations, isolations, and purification steps.[76–91]

Organo-Brønsted acids, e.g., BINOL-phosphoric acid based on **4**, are privileged catalysts. Symptomatic of their use is N-substituted imine protonation and activation, a widely employed strategy for lowering the lowest unoccupied molecular orbital energies of C=N bonds while increasing their susceptibility to nucleophilic attack. With this tactic, racemic or optically active non-isotope-enhanced aziridines can be generated from alkyl diazoacetates and in situ synthesized or preformed N-substituted imines.[92–97] Given the widespread and operational simplicity of organo-Brønsted acid "imine activation," it is somewhat surprising that an isotope-incorporating variant of the aza-Darzens reaction has not been reported.

Initiating our research, we screened organocatalysts **4**–**8** for their ability to "activate" imine **9** by allowing its reaction with α-[2H]-diazoester **10** or **11**[98] and thus afford [2H]C_2-**12** (R = Et or ^{t}Bu; Figure 4). Incorporating the 2-pyridyl group within

(*E*)-1-phenyl-*N*-(pyridyl-2-ylmethylene)methanamine **9**, we surmised that protontransfer from **4**–**8** would generate an intramolecular bifurcated hydrogen bond[99–102] between the two sp^2 nitrogens and afford an optically active and electrophilic immonium ion pair (**13**). Our rationale for this approach, and its potential benefits, originated from published density functional theory (DFT) calculations (BHandHLYP method) on an asymmetric Mannich reaction that indicated that a bifurcated hydrogen bond was able to activate and create a rigid optically active environment around an *N*-(2-hydroxyphenyl)-derived imine.[103] Disappointingly, **4**–**8** were unable to activate **9**, and no reaction was observed. Indeed, **9** was returned with good mass balance even when (1) the reaction was performed neat, i.e., [2H]-**10** was the solvent; (2) the reaction occurred in the presence of 4 Å molecular sieves to remove any potentially detrimental trace amounts of water; (3) **4**–**8** were left for 120 hr at ambient temperature and subsequently at an elevated temperature, rescinding the possibility of a slow reaction; (4) **4**–**8** were increased to 20 mol %, negating the possibility that they had poor catalyst turnovers; and (5) a series of solvents with diverse dielectric properties were investigated in a search for a strong "solvent effect." All to no avail.

Failure to generate a sufficiently activated form of **9** could have been associated with the relatively low p*K*a of **4**–**8**, i.e., ~13 in MeCN. On the contrary, (*R*)- and (*S*)-BINOL *N*-triflylphosphoramides (**14**) are, as outlined in Figure 4, considerably more reactive and acidic (p*K*a of ~6.5 in MeCN).[104] As a consequence, these have widespread application[105–119] and are currently the tour de force of the organo-Brønsted acid catalysis world. Independently reacting [2H]-**10** or [2H]-**11** ([2H] > 95 atom %) with (*E*)-1-phenyl-*N*-(pyridyl-2-ylmethylene)methanamine **9** in the presence of (*S*)-**14** (Ar = Ph, 10 mol %) for 12 hr at ambient temperature consumed both reactants. ^{1}H-NMR analysis of the two unpurified reactions indicated that **12** (R = Et or ^{t}Bu) had been generated cleanly and efficiently (no enamine). The unoptimized yields were good (78% for R = Et and 71% for R = ^{t}Bu), and the absence of the characteristic doublet in both ^{1}H-NMR spectra at ~2.6 ppm[120] (associated with the aziridine proton, i.e., HC-CO_2Et or ^{t}Bu) confirmed excellent levels ([2H] > 95 atom %) of regiospecific [2H]-incorporation on C_2 of **12**; no evidence for isotope scrambling was observed. The excellent levels of [2H]-incorporation on C_2 verified several important points: (1) during the reaction, the deuterium on [2H]-**10** and [2H]-**11** did not undergo [1H] ⇄ [2H] exchange; (2) once "installed" on **12**, the deuterium on C_2 did not scramble onto, for example, the [2H]C_3 position; and (3) (*S*)-**14** did not promote [1H] ⇄ [2H] exchange in aziridine **12** or alkyl α-[2H]diazoacetate [2H]-**10** or [2H]-**11**.

Disappointingly, chiral column high-performance liquid chromatography (HPLC) analysis established that aziridines **12** (R = Et or ^{t}Bu) were racemic. So, although we were delighted that (*S*)-**14** (Ar = Ph) catalyzed the synthesis of **12**, its formation as a racemic mixture was frustrating. Completing a comprehensive reaction condition, a substrate, solvent, and catalyst screening program established that at −80°C (*E*)-2-(*tert*-butoxy-*N*-pyridin-2-ylmethylene)aniline **15** reacted with [2H]-**11**. Although the reaction can be successfully conducted in various solvents, for catalyst-optimization studies we chose a combination of [2H]chloroform/dichloromethane (8:2 v/v) as a convenient solvent mixture because it allowed ^{1}H-NMR monitoring of the reactions. Screening a wide array of catalysts, we eventually settled on "sterically tuned" 3,3′-anthracenyl-(*S*)-**17** (10 mol %), which afforded [2H]C_2-**16** (Figure 4) in an 82% yield and, importantly, an excellent 99% enantiomeric excess (ee). ^{1}H-NMR analysis and careful integration of the signals associated with *tert*-butyl 1-(2-*tert*-butoxyphenyl)-3-(pyridin-2-yl)-[2H]C_2-aziridine-2-carboxylate (**16**) confirmed regiospecific [2H] > 95 atom % at C_2 (see Figures S1 and S2).

Table 1. Organo-Brønsted-Acid-Catalyzed Synthesis of Optically Active [2H]C_2-21–[2H]C_2-32

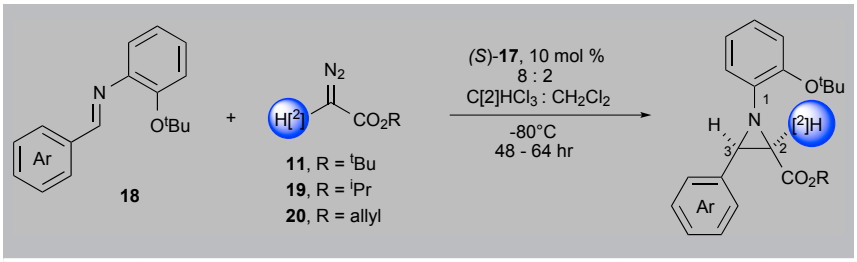

Number	Aryl Group (Ar)	R Group	Yield (%)	ee
21	phenyl	*tert*-butyl	65%	81%
22	2-naphthyl	*tert*-butyl	85%	99%
23	4-chlorophenyl	*tert*-butyl	55%	67%
24	4-bromophenyl	*tert*-butyl	87%	95%
25	4-fluorophenyl	*tert*-butyl	65%	80%
26	pentafluorophenyl	*tert*-butyl	82%	97%
27	4-nitrophenyl	*tert*-butyl	95%	90%
28	4-cyanophenyl	*tert*-butyl	65%	99%
29	4-fluorenylmethyloxycarbonate	*tert*-butyl	78%	92%
16	2-pyridyl	*tert*-butyl	82%	99%
30	2-pyridyl	*iso*-propyl	78%	92%
31	4-cyanophenyl	*iso*-propyl	80%	96%
32	4-cyanophenyl	allyl	68%	90%

For synthesis, see Figures S4–S15.

We next undertook a substrate study incorporating an array of preformed structurally and functionally diverse *N*-(2-*tert*-butoxyphenyl)imines based on **18** (Table 1), sterically demanding [2H]-**11**, and catalyst (*S*)-**17**. Employing preformed imines rather than generating them in situ assured us that any lack of reaction or low yield was not associated with slow or incomplete *N*-(2-*tert*-butoxyphenyl)imine formation at −80°C. We confirmed the utility of (*S*)-**17** to mediate the efficient synthesis of [2H]C_2-labeled aziridines by incorporating a diverse array of unfunctionalized monocyclic aromatic (e.g., benzaldehyde), multicyclic aromatic (e.g., 2-naphthaldehyde), and substituted aromatic (e.g., 4-chloro, 4-bromo, 4-fluoro, pentafluoro, 4-nitro, 4-cyano, 4-(*O*-Fmoc)phenyl) carboxaldehydes, as well as heterocyclic 2-pyridinecarboxaldehyde. All were successfully synthesized in good (55%) to excellent (97%) yields and, in the majority of examples, excellent ee (90%–99%); see, for example, **16** and **22**–**29** in Table 1 (and Figures S5–S19). Furthermore, incorporating the sterically less demanding isopropyl ([2H]-**19**) or allyl ([2H]diazoacetate [2H]-**20**) afforded [2H]C_2-**30**–[2H]C_2-**32** in good yields and excellent (90%–96%) ee. Importantly, universally excellent regiospecific [2H] > 95 atom % incorporation at the C_2-atom, as determined by ^{1}H-NMR (see Figures S20–S24) and mass spectrometry molecular and fragment ion analysis, was observed for [2H]C_2-**21**–[2H]C_2-**32** and was directly related to the isotopic enrichment employed in starting materials **11**, **19**, and **20**. Substantiating this, the ^{1}H-NMR spectrum of [2H]C_2-**21** (see Figures S3 and S4) confirmed that the characteristic doublet associated with the proton on C_2 at 3.1 ppm had disappeared with concomitant formation of a broad singlet at 3.4 ppm associated with the proton on C_3. This observation was general and consistent for all ^{1}H-NMR spectra of [2H]C_2-**21**–[2H]C_2-**32**, albeit the chemical shifts of individual C_3-protons varied slightly. *cis*-Diastereoselectivity had been tentatively assigned to the

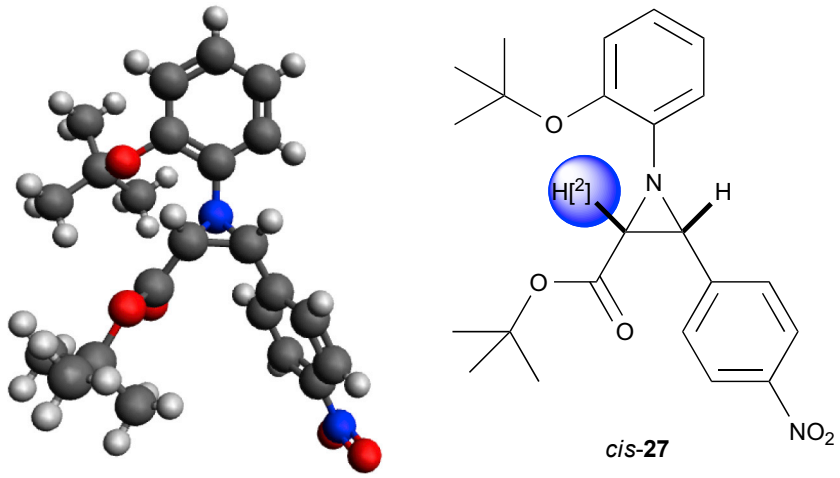

Figure 5. X-Ray Crystal Structure of Optically Active, [2H]C_2-Labeled *cis*-$C_{2,3}$-Disubstituted 27

$C_{2,3}$-substituents on [2H]C_2-**21**–[2H]C_2-**32**. Confirmation of this assignment was essential. Subjecting a crystal of [2H]C_2-**27** to X-ray analysis (Figure 5) clearly showed the *cis*-diastereoselective relationship between the *tert*-butoxycarbonyl and 4-nitrophenyl substituent, as well as their *trans*-relationship with the *N*-(2-*tert*-butoxyphenyl) group attached to the nitrogen of the aziridine (see Accession Numbers).

Preliminary results indicate that (*S*)-**17** is an excellent activator of preformed *N*-(2-*tert*-butoxyphenyl)imines, given that it induced very good levels of diastereo- and stereoselectivity within a diverse array of *N*-(2-*tert*-butoxyphenyl)-$C_{2,3}$-disubstituted [2H]C_2-aziridines. Confident that our methodology was robust, we focused our attention on the *cis*-diastereo- and stereoselective synthesis of [2H]C_3-aziridinyl alkyl esters via an operationally simplified one-pot, three-component, two-step protocol employing 2-*tert*-butoxyaniline (**34**), aryl [2H]aldehydes (e.g., **33**, [2H] > 95 atom %), and natural-isotope-abundant ([2H] = 0.0156%) alkyl diazoesters. Probing this, we reacted commercially available α-[2H]-benzaldehyde (^{2}H > 98 atom %), 2-*tert*-butoxyaniline (**34**; Table 2), *tert*-butyl α-diazoacetate (**35**), and organo-Brønsted acid (*R*)-**17** (10 mol %). Gratifyingly, [2H]C_3-**36** was afforded in an unoptimized 65% yield and 88% ee; these values compare favorably with those derived from (*S*)-**17** for the synthesis of [2H]C_2-**21** (65% yield and 81% ee; Table 1). No isotope scrambling was observed, and [2H]C_3-**36** was afforded with >95 atom % deuterium incorporation at C_3. A series of functionalized aryl α-[2H]aldehydes ([2H] > 95 atom %) based on **33** were readily synthesized by a slightly modified procedure originally reported by Curley et al.[121] Reacting these with 2-*tert*-butoxyaniline **34**, *tert*-butyl α-diazoacetate **35**, and (*R*)-**17** (10 mol %) in our standard one-pot, multi-component, two-step protocol afforded [2H]C_3-aziridines **37**–**43**; chiral column HPLC analysis confirmed that they had been generated with high to excellent ee. Furthermore, Table 2 demonstrates that universally excellent regiospecific [2H] > 95 atom % incorporation at the C_3-atom was observed for [2H]C_3-**37**–[2H]C_3-**43**. These preliminary results have established two viable synthetic routes to [2H]C_2- and [2H]C_3-aziridines with either preformed *N*-(2-*tert*-butoxyphenyl)imines or the operationally more straightforward one-pot, multi-component, two-step protocol. Both afford, within experimental error, identical results. Furthermore, switching between the enantiomeric forms of catalyst **17** and translocating the deuterium atom from the formyl group of the aldehyde to the α-diazoester had little effect on

Table 2. Organo-Brønsted-Acid-Catalyzed Synthesis of Optically Active [2H]C_3-36–[2H]C_3-45

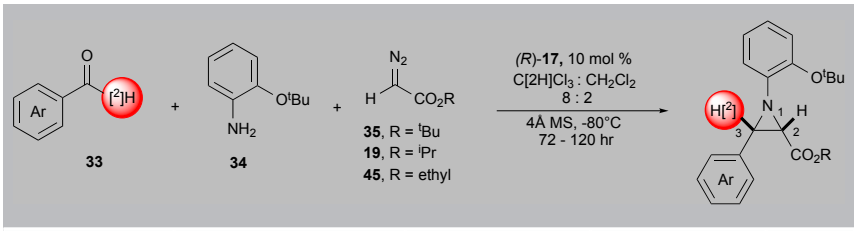

Number	Aryl Group (Ar)	R Group	Yield (%)	ee
36	phenyl	*tert*-butyl	65%	88%
37	4-bromophenyl	*tert*-butyl	67%	83%
38	4-fluorophenyl	*tert*-butyl	72%	86%
39	4-chlorophenyl	*tert*-butyl	67%	71%
40	3-chlorophenyl	*tert*-butyl	67%	69%
41	2-chlorophenyl	*tert*-butyl	41%	64%
42	4-cyanophenyl	*tert*-butyl	41%	90%
43	4-nitrophenyl	*tert*-butyl	53%	93%
44	4-bromophenyl	*iso*-propyl	65%	84%
45	4-bromophenyl	ethyl	52%	74%

For synthesis, see Figures S16–S24.

the yield, enantioselectivity, or percentage of deuterium incorporation. The reaction times for producing [2H]C_3-**36**–[2H]C_3-**45** (see Figures S25–S44) via the one-pot, three-component, two-step protocol were longer than those for generating [2H]C_2-**21**–[2H]C_2-**32** via non-isotope-enhanced preformed aryl *N*-(2-*tert*-butoxyphenyl)imines. It seemed unlikely that the slower reaction rate affording [2H]C_3-**36**–[2H]C_3-**45** could be attributed to a significant secondary kinetic isotope effect.[122] Instead, a more likely explanation was associated with the slow rate of aryl *N*-(2-*tert*-butoxyphenyl)-[2H]-imine formation at −80°C with the sterically encumbered 2-*tert*-butoxyaniline. A mixture of α-diazoester **35** and pre-synthesized (*E*)-*N*-(4-nitro-[2H]-benzylidene)-2-*tert*-butoxyaniline was cooled to −80°C, and (*R*)-**17** (10 mol %) was subsequently added.

Consistent with previous chemistry outlined in Table 1 (affording (stereo)isotopomer [2H]C_2-**27** from the corresponding non-isotopically-labeled imine), aziridine [2H]C_3-**43** was afforded in 48 hr with a similar yield and ee to [2H]C_2-**27**. In a demonstration of ee reproducibility between different isotopologue syntheses (Tables 2 and 3), it is noteworthy that **21** and **36** (both Ph), **23** and **39** (both 4-chlorophenyl), **25** and **38** (both 4-fluorophenyl), **27** and **43** (both 4-nitrophenyl), and **28** and **42** (both 4-cyanophenyl) afforded, within experimental error, very similar ee values. To further exemplify the utility of our methodology, particularly the ease with which multiple deuterium atoms can be established into optically active aziridines, we wanted to generate the first example of an organo-Brønsted-acid-catalyzed stereoselective reaction that installed two deuterium atoms. α-[2H]Benzaldehyde, 2-*tert*-butoxyaniline, and *tert*-butyl α-[2H]diazoacetate (Table 3) were mixed at −80°C in the presence of (*R*)-**17** (10 mol %). [2H]C_2-[2H]C_3-**46** was afforded in a 72% yield and 67% ee. Furthermore, ^{1}H-NMR indicated >95 atom % incorporation at both C_2- and C_3-aziridine positions. This key result convinced us of the merits of generating additional examples. 4-Bromophenyl-[2H]C_2-[2H]C_3-**47**, 4-fluorophenyl-[2H]C_2-[2H]C_3-**48**, and 4-nitrophenyl-[2H]C_2-[2H]C_3-**50** were all afforded with excellent levels of deuterium incorporation, i.e., >95 atom % at both C_2- and C_3-centers.

Table 3. Organo-Brønsted-Acid-Catalyzed Synthesis of Optically Active [2H]C_2-[2H]C_3-46–[2H]C_2-[2H]C_3-53

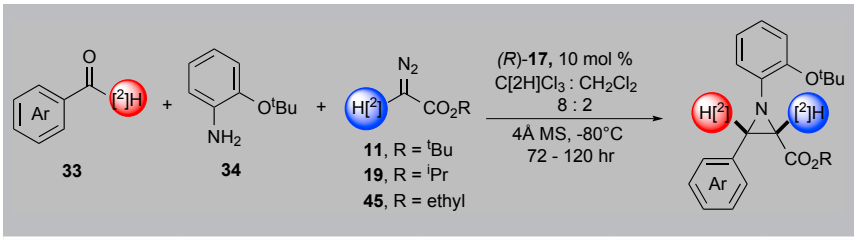

Number	Aryl Goup (Ar)	R Group	Yield	ee
46	phenyl	*tert*-butyl	72%	67%
47	4-bromophenyl	*tert*-butyl	76%	92%
48	4-fluorophenyl	*tert*-butyl	69%	91%
49	4-chlorophenyl	*tert*-butyl	65%	77%
50	4-nitrophenyl	*tert*-butyl	57%	97%
51	4-bromophenyl	*iso*-propyl	76%	87%
52	3-chlorophenyl	*tert*-butyl	58%	76%
53	2-chlorophenyl	*tert*-butyl	51%	52%

For synthesis, see Figures S25–S33.

Furthermore, HPLC analysis confirmed excellent levels of asymmetric induction: 92% ee for [2H]C_2-[2H]C_3-**47**, 91% ee for [2H]C_2-[2H]C_3-**48**, and 97% ee for [2H]C_2-[2H]C_3-**50**. Similar to our previous application, using isopropyl α-[2H]diazoacetate (cf. 4-bromophenyl-[2H]C_3-**44** in a 65% yield and 84% ee) afforded isopropyl ester [2H]C_2-[2H]C_3-**51** in an improved 76% yield and slightly higher 87% ee. As with previous examples, universally excellent regiospecific [2H] > 95 atom % incorporation at the C_2- and C_3-atom was observed for [2H]C_2-[2H]C_3-**46**–[2H]C_2-[2H]C_3-**53** (see Figures S45–S60).

Comparing the ee values associated with C_3-(3-chlorophenyl) [2H]C_3-**40** (69% ee; Table 2) and [2H]C_2-[2H]C_3-**52** (76% ee; Table 3) with those of [2H]C_2-**21**–[2H]C_2-**22** (81% and 99% ee, respectively), [2H]C_2-**24**–[2H]C_2-**32** (80%–99% ee; Table 1), [2H]C_3-**37**–[2H]C_3-**38** (83% and 86% ee, respectively), and [2H]C_3-**42**–[2H]C_3-**45** (74%–93% ee; Table 2) provides evidence that the 3-chlorophenyl group generates aziridines with reduced ee. Similarly, incorporating a C_3-(2-chlorophenyl) group afforded [2H]C_2-[2H]C_3-**53** and [2H]C_3-**41** with lower ee (i.e., 52% and 64%, respectively) than, for example, C_3-(4-chlorophenyl)-, (4-bromophenyl), or (4-fluorophenyl)-derived [2H]C_2-[2H]C_3-**49**–[2H]C_2-[2H]C_3-**52** (77%–97% ee; Table 3). Currently, it is unclear why the 2-chlorophenyl- and 3-chlorophenyl-afford lower ee than the halide-derived examples above or pentafluoro-[2H]C_2-**26** (97% ee); it does, however, seem specifically related to the inclusion of a 2- or 3-chlorophenyl and is not solely a consequence of the electronegativity of chlorine.[123]

Having established a preference for catalyst **17** to afford *cis*-aziridines, we sought a tentative mechanistic rational to help explain their formation. Protonation, (*S*)-**17**, of the *N*-arylimine nitrogen attached to the bulky *ortho*-*tert*-butoxyaryl substituent (**54**) affords electrophilic immonium ion pair **55** and a five-membered intramolecular hydrogen-bonded immonium complex. Minimizing steric interactions (see highlighted red structures on **57**) of the bulky *tert*-butyl α-[2H]diazoacetate toward ion pair **55** preferentially affords **56**. Alternative approaches of the *tert*-butyl α-[2H]

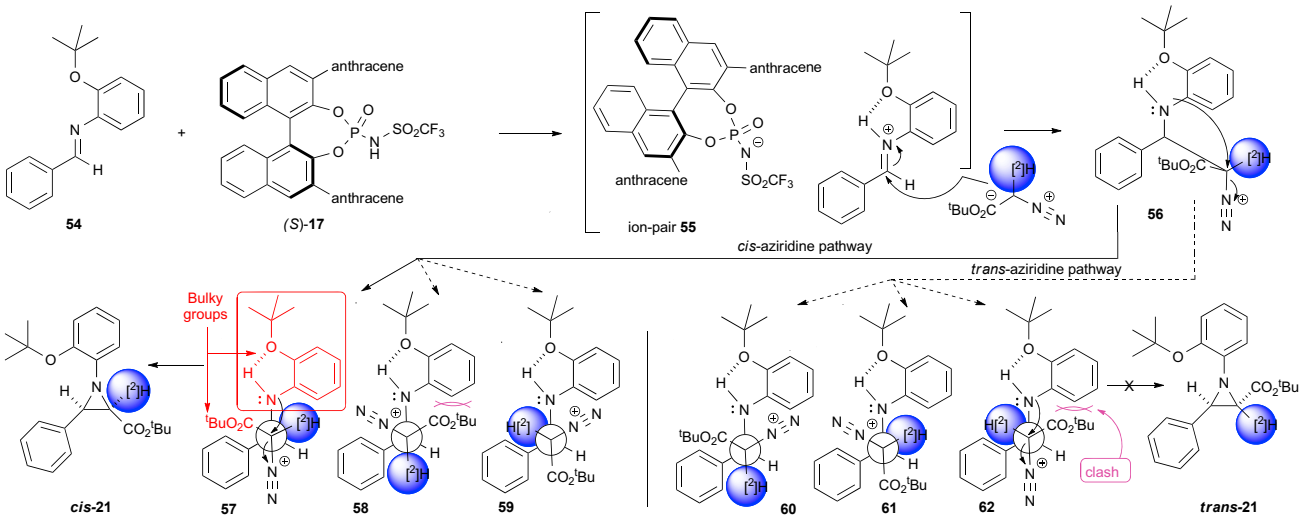

Scheme 1. Potential Mechanistic Rational Model for the Synthesis of Optically Active [2H]C_2-21

diazoacetate proceed via intermediates with increased steric congestion (**58**, a clash between *tert*-butyl ester and bulky *N*-aryl group) or require 120° rotation around the newly formed central C–C bond of **59** so that the $-N_2$ leaving group is in a suitable orientation for S_N2 displacement and ring closure (**57**) via nucleophilic attack of the aryl nitrogen atom (Scheme 1). The preference for generating *cis*-aziridines instead of *trans*-aziridines is interesting and worthy of comment.[124] Similar to *cis*-**21**, Newman projections **60**–**62** (Scheme 1) present a clearer understanding of why this is the case. Generating *trans*-**21** requires that the diazo leaving group be anti-periplanar to the incoming nucleophilic aryl nitrogen; however, as outlined in **62**, this conformation results in a severe clash between the bulky *tert*-butyl ester and the N-bound *ortho*-*tert*-butoxyaryl group. This results in a transition state with increased energy, and consequently *trans*-**21** is not generated. In contrast, although **60** and **61** (Scheme 1) have reduced steric interactions, both conformations have the diazo leaving group in the wrong conformation (not anti-periplanar to the incoming arylamine nucleophile). Indeed, the only way that **60** and **61** can afford *trans*-**21** is via a 120° clockwise (**60**) or anti-clockwise (**61**) rotation around the central C–C bond.

However, doing this only serves to re-establish the severe steric interactions observed in **62**; consequently, **60** and **61** are unlikely to be efficient pathways to *trans*-**21**. A comprehensive mechanistic and computational study that fully explains the stereoselectivity observed with triflimide (*S*)-**17** or (*R*)-**17** has yet to be undertaken. However, using high-level quantitative ONIOM (Our Own N-layered Integrated Molecular Orbital and Molecular Mechanics) calculations, Goodman et al. developed a BINOL-derived phosphoric acid (based on **4**; Figure 4) model that helps explain the observed stereoselectivities when nucleophiles add to imines.[125] Extrapolating the Goodman bifunctional phosphoric acid imine activation model by substituting a triflimide group for the hydroxyl group of the phosphoric acid affords a quadrant model that projects the catalyst with the BINOL oxygens in the plane of the paper (blue bonds and atoms, **63**; Scheme 2), the triflimide above (pink atoms and bonds), and the P=O group below (red bonds and atoms), each with the bulky 3- and 3′-aryl groups on either side. *E*-imines (e.g., **54**; Scheme 1) are more stable than *Z*-imines; consequently, aldimines have a larger energy difference between the *E*- and *Z*-forms.

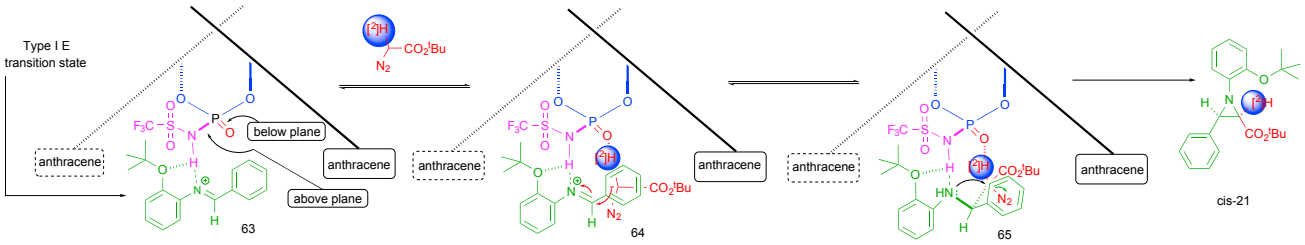

Scheme 2. Proposed Transition-State Model for the Synthesis of Aziridine *cis*-21

Reaction of complex (*S*)-**17**-with imine **54** generates optically active immonium complex **63**; subsequent co-ordination of *tert*-butyl α-[2H]diazoacetate produces **64** and then **65**, and finally, cyclisation affords *cis*-**21**.

Although a type I *Z*-transition state (data not shown) is more compact, the energy required to rotate the *ortho*-*tert*-butoxyphenyl is greater than the energy of the steric interactions with the large 3,3′-substituents. With this in mind, we propose that, similarly to **63**, **54** generates an activated type I *E*-hydrogen-bonded transition-state complex (Scheme 2) with the bulky *ortho*-*tert*-butoxyaryl group projecting into the left-hand empty quadrant. Binding the *tert*-butyl α-[2H]diazoacetate to the P=O within the second vacant quadrant aligns the nucleophile directly below the activated imine double bond of **63**, affording a complex similar to **64**. Stereoselective attack of the α-[2H]diazoacetate generates a new optically active C–C bond with the diazo leaving group anti-periplanar to the arylamine group; subsequent cyclisation affords the desired optically enhanced aziridine *cis*-**21**.

By exploiting the quadrant model (**66**, Figure 6) and incorporating new catalysts, it could be possible to increase the stereoselectivity and/or rate of the aza-Darzens reaction. As noted, activating the imine of **9** with phosphoric acid **4** (p*K*a = 3.15 in DMSO) was not possible. Replacing it, however, with the more acidic (*S*)-**17** (p*K*a = −3.36 in DMSO) activated the imine and afforded the *cis*-aziridines. Thus, testing second-generation, more acidic catalysts such as **67** (p*K*a −3.83 in DMSO) and **68** (p*K*a −4.58 in DMSO; Figure 6) will allow the important aspect of p*K*a to be probed. Similarly, incorporating TRIP-derived *N*-triflimide **69** and sulfur- and selenium-substituted *N*-triflimides **70** and **71** (anticipated to have similar a p*K*a to **67** and **68**) will allow investigation of the effect that larger 3- and 3′-substituents have on the stereoselectivity and reaction rate. Furthermore, Yamamoto and Sai[126] recently reported an asymmetric Hosomi-Sakurai reaction catalyzed by **72**; improved diastereo- and enantioselectivity was attributed to the incorporation of the perfluoroalkyl tether and the bulky *tert*-butyldiphenylsilyl groups, which increased the steric bias within the filled quadrants I and IV (**66**; Figure 6). Exploiting this, synthesizing aziridines with increased optical activities via enhanced reaction rates by using lower catalyst loadings seems viable.

Optically active α- and/or β-deuterated natural and unnatural α-amino acids are important (bio)chemical motifs (see Figures 2H–2P) mainly generated via multi-step, enolate-based chemistry using Schöllkopf *bis*-lactim ethers, Evans oxazolidinones, Williams' oxazoline, Oppolzers' sultam, or Seebach imidazolidinone chiral auxiliaries.[127–141] The development of an operationally simple, catalysis-based protocol that transforms easily accessible starting materials into *cis*-aziridines "en route" to natural or unnatural, optically active, isotope-enhanced α-amino acids holds considerable merit. Isotope-enhanced α-amino acids are valuable bioprobes that have been used for investigating protein-protein interactions,[142] identifying unknown compounds from orphan gene clusters (the so-called genomisotopic approach),[143] and determining the metabolic

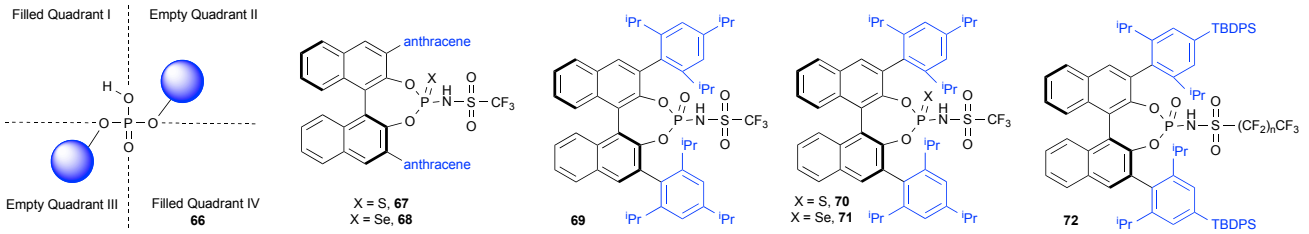

Figure 6. Alternative, More Reactive Organo-Brønsted Acids for the Synthesis of Isotope-Enhanced *cis*-Aziridines

and conformational stabilities[144] of proteins and peptides.[145] Preliminary hydrogenation studies using catalytic quantities (20 mol %) of palladium hydroxide on carbon (20 mol % Pd on C) focused on [2H]C_2-**21** (Table 1) and [2H]C_2-[2H]C_3-**46** (Table 3). Optically active *N*-aryl phenylalanine *tert*-butyl ester α-[2H]-**73** (Figures S61 and S62) and α-[2H]- and β-[2H]-**74** (Figures S63 and S64) were afforded in excellent 93% and 90% yields, respectively (Figure 7). It is worth noting that there was with little evidence (^{1}H-NMR) for loss of the deuterium or erosion of the optical activity incorporated via the asymmetric aza-Darzens reaction. Analytical chiral column HPLC analysis confirmed that α-[2H]-**73** and α[2H]-,β-[2H]-**74** had 80% and 70% ee, respectively. These values match, within experimental error, those of the starting-material aziridines (e.g., [2H]C_2-**21** had 81% ee, and [2H]C_2-[2H]C_3-**46** had 67% ee). Thus, under the mild, closely monitored hydrogenation conditions, these substrates did not undergo "deuterium washout." Encouraged by this, we sought to expand our repertoire such that it included multicyclic, heteroaryl, and haloaryl α-[2H]-, β-[2H]-, and α-[2H],β-[2H]-α-amino acids. Hydrogenating (2-naphthyl)-[2H]C_2-**22** and (2-pyridyl)-[2H]C_2-**16** (both 99% ee and [2H] > 95 atom %) afforded *N*-(2-*tert*-butoxyphenyl) *tert*-butyl esters of 3-(2-naphthyl)-α-[2H]-alanine[146–148] (**75**) and unnatural 3-(2-pyridyl)-α-[2H]-alanine[149] (**76**) in 80% and 64% yields, respectively (Figure 7). Importantly, both retained their excellent levels of deuterium incorporation (>95 atom %), and chiral column HPLC analysis established that they had 77% and 97% ee, respectively (Figures S65–S68).

The synthesis of unnatural β-(aminoaryl) and β-(haloaryl) α-amino acids, e.g., **77** and **78**, respectively, (Figure 7), is an important endeavor worthy of investigation.[150–160] Only three isotope-enhanced 4-aminophenylalanines[161,162] have been reported. Two of these detail the deuterium incorporation within the side chain groups—not, as would be preferable, at one or both of the α- or β-carbons on the α-amino propanoic acid chain (see α-[2H]-β-[2H]-**93**–β-[2H]-**95** in Scheme 3).[163] To increase atom efficiency, we envisaged executing a one-pot, double-reduction process whereby the Baeyer strain in [2H]C_2-**27** is released while the 4-nitrophenyl is reduced to a 4-aminophenyl group. In a reaction employing previously successful conditions and palladium catalysts, 4-nitrophenyl derived [2H]C_2-**27**, [2H]C_3-**43**, and [2H]C_2-[2H]C_3-**50** underwent "global" hydrogenation, affording the desired 4-aminophenyl-derived α-amino esters α-[2H]-**77**, β-[2H]-**78**, and α-[2H]-β-[2H]-**79** in 85%, 97%, and 82% yields and 86%, 89%, and 94% ee, respectively (Figures S69–S74). The ee values are, within experimental error, identical to those of the starting materials. Demonstrating the utility of multi-isotope-derived unnatural 4-aminophenyl α-amino acids based on α-[2H]-**77**–α-[2H]-β-[2H]-**79**, Herbert and Knaggs exploited *rac*-**90** as a biosynthetic probe for the β-lactam antibiotic obafluorin;[161] *rac*-**90** helped to establish that the biosynthetic route did not proceed via a pyridoxal-phosphate-mediated decarboxylation.

Halophenyl- and especially fluorophenyl-derived[164–171] α-amino acids are important motifs widely employed in medical chemistry to generate "Teflon" proteins or help

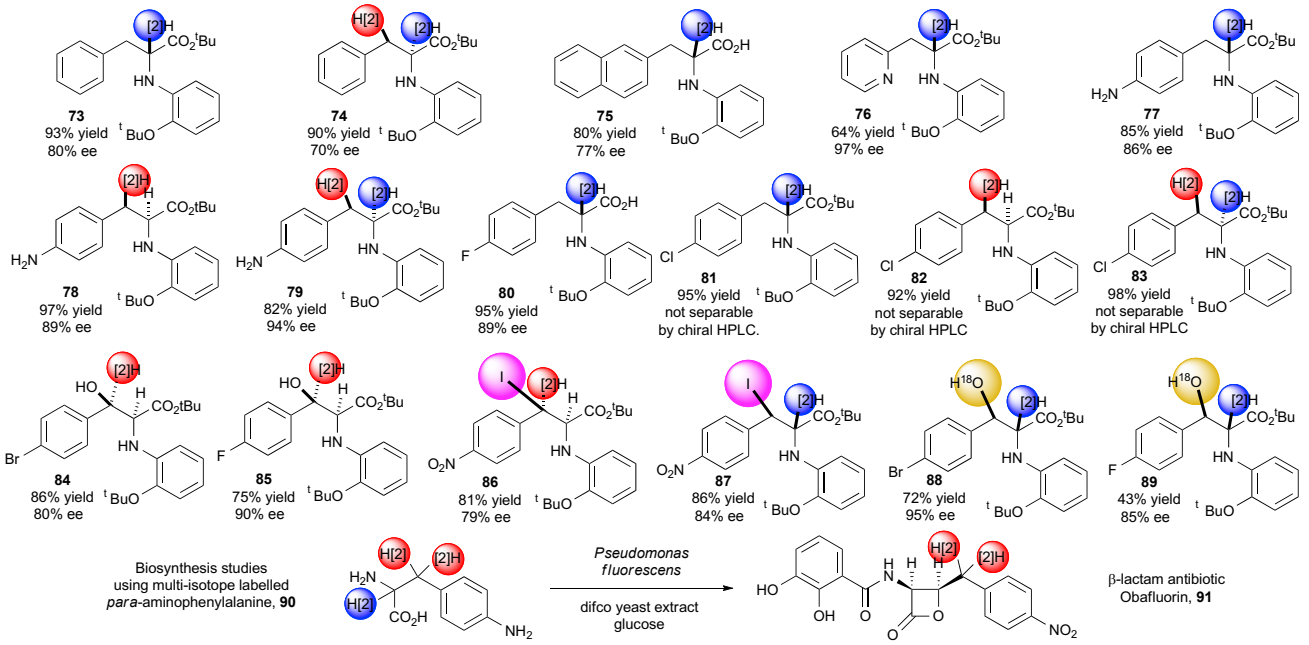

Figure 7. Synthesis of Isotope-Enhanced α-Amino Carboxylic Esters and β-Substituted-α-amino Carboxylic Esters
For synthesis, see Figures S34–S51.

stabilize tertiary and quaternary protein structures. Hydrogenating (4-fluorophenyl)-[2H]C_2-**25** afforded the corresponding ring-opened *tert*-butyl ester α-amino acid (data not shown) in an excellent 95% yield and >95 atom % deuterium at the C_2-site. Determining its optical purity was not possible by chiral column HPLC analysis; the corresponding racemic sample was not separable. However, chemoselective hydrolysis of the *tert*-butyl ester with formic acid afforded carboxylic acid α-[2H]-**80**.

β-Hydroxy-α-amino acids are key components of important bioactive natural products, e.g., vancomycin (antibacterial), bouvardin (anticancer), orenticin (antibacterial), phomopsins (mycotoxin), ristocetin (antibiotic), and actaplanin (antibiotic). Furthermore, they are also essential building blocks for the synthesis of β-lactams, β-fluoro-α-amino acids, and carbohydrates. Consequently, many examples of asymmetric synthesis strategies afford non-isotope-enhanced β-hydroxy-β-aryl-α-amino acids. A non-exhaustive list includes lithium amide conjugate addition,[172] transition-metal-mediated hydroborylations,[173] the use of chiral auxiliaries (i.e., oxazolidinones,[174] oxazolines,[175] and *bis*-lactim ethers[176]), and substrate-specific biocatalysis.[177–180] And yet, despite this intensive research effort, only two reports have detailed the synthesis of α-[2H]-, β-[2H]-, and α-[2H]-β-[2H]-β-hydroxy-β-aryl-α-amino acids (Scheme 3). Thus, Hamada et al. reported a deuterium-incorporating mechanistic study that employed a dynamic kinetic resolution (DKR) reaction mediated by a cationic Ir-(*S*)-MeO-BIPHEP complex and pre-deuterated β-keto-α-[2H]-α-amino carboxylate ester **92** (Scheme 3). The DKRs were stopped at low conversions to product to minimize complications caused by hydrogen-solvent deuterium exchange. Be that as it may, hydrogenation afforded a, presumably inseparable, 1:1.1 mixture of *anti*-α-[2H]-β-[2H]-β-**93** and *anti*-α-[2H]-β-hydroxy-α-amino acid **94**. Interestingly, because hydrogenation of the ketone on α-[2H]-**92** proceeds via enol tautomerization, when deuterium gas was substituted for hydrogen and non-isotope-enhanced acetic acid was used, mono-deuterated isotopologue β-[2H]-**95** was afforded together with naturally abundant *anti*-β-hydroxy-α-amino acid **96** in a 1:1.4 mixture (the article does not say whether they were separable).

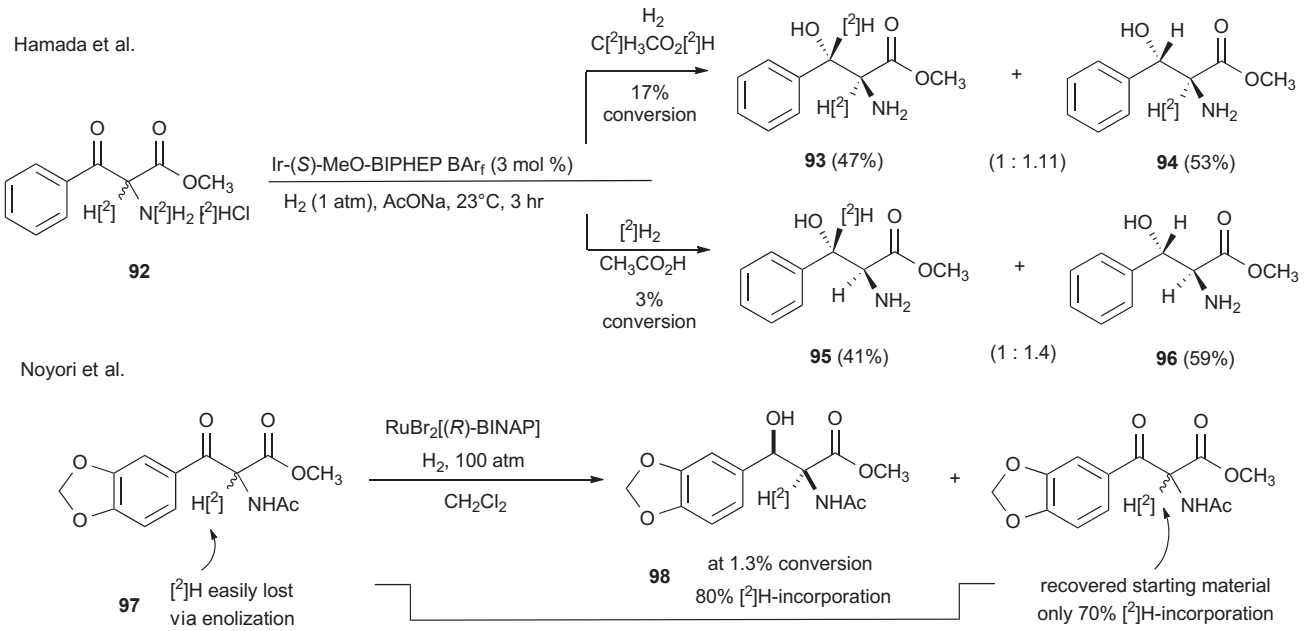

Scheme 3. Synthesis of Deuterium Incorporating β-Hydroxy-β-aryl-α-amino Acids 93–95 and 98

In early mechanistic studies on asymmetric hydrogenation, Noyori et al. generated *syn*-α-[2H]-β-hydroxy-β-aryl-α-amino acid **98** by using $RuBr_2$[(*R*)-BINAP] and, again, a pre-deuterated β-keto-α-[2H]-β-aryl-α-amino acid, **97**. Worthy of note, Noyori reported that "2-deuterio **97** easily loses deuterium via enolization" and that conducting the hydrogenation at a very low 1.3% conversion afforded α-[2H]-β-hydroxy-β-aryl-α-amino acid **98** with only 80% [2H]-incorporation (ee not reported). Furthermore, and of particular concern, recovered **97** had significantly reduced (70%) deuterium incorporation. In summary, neither of these transition-metal-based methods is particularly suited to bespoke isotope incorporation; instead, they afford presumably inseparable isotopologues of β-hydroxy-β-aryl-α-amino acids with relatively poor levels of isotope incorporation.[181,182]

The potential for exploiting an organo-Brønsted-acid-promoted hydrolytic ring opening of isotope-labeled aziridines offered an alternative (cf. Scheme 3), efficient, operationally straightforward entry point to these high-value entities. Employing cheap "off the shelf" 4-toluenesulfonic acid (PTSA), aqueous acetonitrile (1:1), and mild reaction conditions readily transformed [2H]C_3-**37** and [2H]C_3-**38** (Table 2) into β-[2H]-**84** and β-[2H]-**85**, respectively (Figure 7), in unoptimized 86% and 75% yields, respectively (Figures S85–S88). Importantly, there was no evidence of deuterium scrambling or reduced incorporation ([2H] > 95 atom %). Furthermore, chiral column HPLC analysis confirmed no erosion of their optical purities. Encouragingly, a conceptually important next step was to reinforce the utility of our methodology by generating unusual, highly functionalized, isotope-labeled, optically active α- or β-[2H]-β-iodo-α-amino esters **86** and **87** (Figure 7). In a slightly modified procedure,[183] [2H]C_2-**27** and [2H]C_3-**43** reacted in 20 min with iodine- and polystyrene-immobilized thiophenol. Gratifyingly, β-iodo-α-amino esters β-[2H]-**86** and α-[2H]-**87** were afforded with >95 atom % deuterium incorporation in unoptimized 81% and 86% yields and 79% and 84% ee, respectively (Figures S89–S92). Further transformation of these benzyl-activated α-amino acids, affording highly functionalized, desirable isotope-labeled building blocks, seems feasible.

Protocols that afford optically active α-amino acid building blocks that are also appended with multiple and identical or differentiated isotopes, such as [2H] and [13C], [2H] and [18O], [2H] and [15N] or [2H], [2H] and [15N] or [2H], and [2H] and [13C], are highly sought after for their physicochemical properties (Figure 1 and Figures 2H–2P). To facilitate uptake of this methodology, it is important to use readily available, easy-to-handle isotope-derived reagents (e.g., [2H] → deuterium oxide and [15N] → [15N] ammonium hydroxide). With this in mind and the straightforward synthesis of β-[2H]-**84** and β-[2H]-**85** (Figure 7), we expanded our isotope "repertoire" by installing a high-value [18O]H group that generated α-[2H]-β-[18O]-hydroxy-α-amino esters. Brønsted-acid-mediated (PTSA) ring opening of [2H]C_2-**24** and [2H]C_2-**25** with readily available H_2[18O] ([18O] > 95 atom %) afforded dual-isotope-differentiated α-[2H]-β-[18O]-hydroxy-derived **88** and **89** in unoptimized 72% and 43%[184] yields (Figures S93–S96) and 95% and 85% ee, respectively (Figure 7). Using NMR to confirm [18O] installation is neither straightforward nor convenient. However, the high-resolution mass spectral analysis of **88** and **89** afforded intense signals at *m/z* 467.1524 and 407.2333, respectively (associated with $[M+H]^+$), thereby confirming that both had [2H]- and [18O]-labeled oxygen (both >95 atom %).

To address the shortfall of aziridines appended with multiple and differentiated isotopes, we considered our isotope "mix and match" approach (Figure 3) to be a simple, effective solution that installs different combinations of [2H], [13C], and [15N]. However, to generate [15N]-labeled *cis*-aziridines with enhanced stereochemical purities, our catalyst-development studies had already established the importance of the 2-*tert*-butoxy group on **34** (Table 2). Yet, our desire to incorporate [15N] with >95% incorporation was frustrated by the lack of a commercial source of [15N]-**34**. For this reason, we opted to expedite our preliminary [15N]-incorporation studies by employing commercially available [15N]aniline (>95 atom %). Using this, we generated four "model" [15N]-aryl substrates: (*E*)-[15N]-(4-nitrobenzylidene) aniline, (*E*)-[15N]-(4-nitro-[2H]-benzylidene)aniline, (*E*)-[15N]-(4-cyanobenzylidene) aniline, and (*E*)-[15N]-(pyridin-2-ylmethylene)aniline (data not shown). Reacting these with [2H]-**11** or **35** in an aza-Darzen reaction mediated by (*S*)-**17** afforded double-differentially labeled [15N]-[2H]C_2-**99**, [15N]-[2H]C_2-**100**, [15N]-[2H]C_3-**101**, and [15N]-[2H]C_3-**102** (Figures S97–S105) with enhanced optical purities and excellent >95 atom % [2H]- and [15N]-incorporation (Figure 8).

A notable isotope milestone we wanted to add to our expanding repertoire of isotopes was [13C] (cf. Figure 1). α-[13C]-Benzoic acid (99 atom% [13C]-incorporation) was transformed into ethyl α-[13C]-3-nitrobenzoate, the ester reduced, and the resulting [13C]aldehyde reacted with [15N]aniline, affording (*E*)-[15N]-(3-nitro-[13C]-benzylidene)aniline (data not shown). Supporting the ease with which additional, different isotopes can be incorporated, *tert*-butyl diazoacetate **35** was switched for [2H]-**11**; the former afforded [15N]-[13]C_3-**103**, and the latter, illustrating the ease with which three isotopes differentially positioned can be "dialed up and locked in," afforded [15N]-[2H]C_2-[13]C_3-**104** (Figures S106–S111). Both were generated via identical protocols, and the products were afforded in essentially equal yields (Figure 8) and >95 atom % [13C]- and [15N]-incorporation. Anticipating that [15N]phenyl-derived [15N]-[13]C_3-**99**–[15N]-[2H]C_2-[13]C_3-**104** might have slightly lower ee values (cf. *ortho*-*tert*-butoxyphenyl-derived **16** [99% ee], **27** [90% ee], **42** [90% ee], and **43** [93% ee]), we were delighted that chiral column HPLC analysis confirmed that our unoptimized [15N]phenyl studies had afforded site-selective, multiple- and differentiated-isotope-derived *cis*-aziridines with 75%–87% ee.

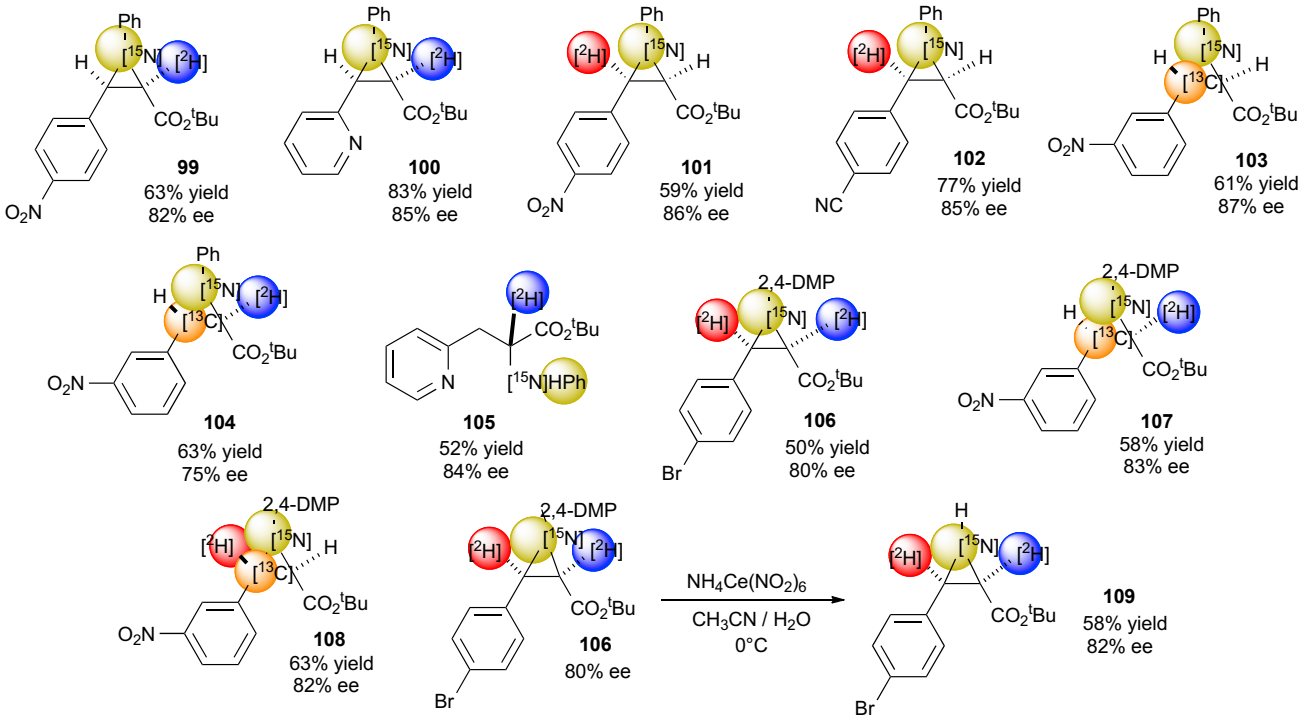

Figure 8. Organocatalytic Synthesis of Optically Active, Labeled [15N]- and $[2H]C_2$- or $[2H]C_3$-99–108 and $[2H]C_2$-$[2H]C_3$-[15N]H-109
For synthesis, see Figures S52–S62.

Bioactive, optically active *N*-aryl α-amino acids equipped with isotopes have been used as PPARγ metabolism probes and for positron emission tomography studies.[185,186] They are generally synthesized by transition-metal-mediated *N*-arylations of α-amino acids or via rhodium carbenoid N-H insertion chemistry. Having established an efficient route to a series of optically active deuterated *N*-aryl α-amino acids, **73–89** (Figure 7), we sought to diversify our approach by generating a straightforward route to isotope-differentiated [15N]aryl α-[2H]-α-amino acids. Establishing that [15N]-inclusion was not detrimental, the efficient hydrogenation of [15N]-$[2H]C_2$-**100** (85% ee) afforded the unnatural [15N]aryl α-amino acid [15N] phenyl-2-pyridyl-α[2H]-alanine *tert*-butyl ester **105** with an 84% ee and >95 atom % for both isotopes. These percentages are, within experimental error, identical to those of the starting material (Figures S112 and S113).

Removing the *N*-aryl substituent, thereby generating optically active multi-isotope-derived NH-aziridines, was also important. Exploiting the ease with which electron-rich *N*-2,4-dimethoxyphenyl (2,4-DMP) groups are cleaved under mild oxidative conditions convinced us of the merits of incorporating [15N]-2,4-dimethoxyaniline. Employing a combination of copper(I) iodide (20 mol %), *L*-proline (40 mol %), and potassium carbonate in aqueous DMSO transformed gram quantities of 1-iodo-2,4-dimethoxybenzene and [15N]ammonium hydroxide (a cheap, commercial source of 98 atom % [15N]) into 2,4-dimethoxy[15N]aniline. Incorporating this and a selection of aryl α-[2H]aldehydes ([2H] > 95 atom %) into our standard protocol afforded isotope-differentiated [15N]-$[2H]C_2$-$[2H]C_3$-**106**, [15N]-$[2H]C_2$-$[13]C_3$-**107**, and [15N]-$[2H]C_3$-$[13]C_3$-**108** in 80%, 83%, and 82% ee, respectively, and >95 atom % for all three isotopes (Figures S114–S123). The 2,4-dimethoxyphenyl group had several beneficial effects: (1) the methoxy groups helped generate the

pre-requisite electron-rich and oxidatively cleavable aryl ring attached to the [15N], and (2) our stereochemical optimization studies (Figure 4) had already identified the importance of increasing the steric bias at the *ortho*-position of the *N*-aryl group (cf. *ortho*-*tert*-butyloxy ether in **15** → **16**; Figure 4). Further confirmation of the positive "*ortho*-effect" was identified in [15N]-[2H]C_2-[13]C_3-**104** and [15N]-[2H]C_2-[13]C_3-**107**; thus, although it is evident that the yields (63% and 58%, respectively) are very similar, the inclusion of the *ortho*-methoxy substituent on **107** results in an increase in ee from 75% to 83%. The 2,4-dimethoxy groups were oxidatively cleaved off [15N]-[2H]C_2-[2H]C_3-**106** with cerium(IV) ammonium nitrate in aqueous acetonitrile. [15N]H-[2H]C_2-[2H]C_3-**109** was afforded in an unoptimized 58% yield. Furthermore, there was no reduction in optical purity, isotope "washout," or scrambling of the deuterium and all isotopes in >95 atom % (Figures S124–S126).

In conclusion, we have developed an exciting approach that allows the installation of single or multiple and identical or different isotopes into a sought-after class of heterocycles. The exceptional ease of our process offers further prospects for isotope incorporation; it uses mild conditions, is operationally straightforward, and is cost effective. Utilizing readily available starting materials and an organo-Brønsted acid catalyst, it transforms, with equal ease, combinations of isotope-enhanced or naturally abundant starting materials into optically active aziridines with site-specific isotope inclusion. Demonstrating the broad utility of our process, the resulting aziridines are readily transformed into isotope-derived, secondary "high-value feedstocks" based on natural or unnatural α- or β-substituted optically active α-amino acids. The future requirements of isotope-derived compounds are increasing; therefore, the design and synthesis of reactions and catalysts that facilitate the incorporation of single or multiple isotopes is almost certainly going to intensify. As the first example of an isotope-incorporating organo-Brønsted acid protocol, we anticipate that our work will open the door to the development of a raft of alternative isoorganocatalytic chemistry. Ultimately, easier access to isotope-labeled compounds will assist chemists and biologists in gaining a better understanding of the fundamental processes associated with the health and well-being research-intensive sectors of the biotech, medtech, agritech, pharmaceutical, and academic communities alike.

EXPERIMENTAL PROCEDURES

Synthesis of 2-(2H)-*tert*-Butyl-1-(2-*tert*-butoxyphenyl)-3-(perfluorophenyl) aziridine-2-carboxylate: 26

Pentafluorobenzaldehyde (40 mg, 0.26 mmol), *O*-*tert*-butoxyaniline (43 mg, 0.26 mmol), and catalyst (*S*)-**17** (22 mg, 0.027 mmol, 10%) were added to a flame-dried Biotage 2 mL microwave vial under nitrogen. 800 μL of [2H]chloroform was added (pre-dried over 4 Å molecular sieves), and the vial was sealed with a polytetrafluoroethylene crimp cap. 200 μL of anhydrous dichloromethane (DCM) was added via syringe through the septum, and the reaction mixture was cooled to −80°C. After 30 min, >95% deuterated *tert*-butyl α[2H]diazoacetate (40 μL, 0.29 mmol) was added via syringe, and the reaction mixture was stirred at −80°C. It was monitored by ^{1}H-NMR until the reaction was deemed complete. At this point, the reaction mixture was passed through a short plug of silica and eluted with diethyl ether. The solvents were removed under reduced pressure, and the residue was purified by flash chromatography (14% diethyl ether in 40°C–60°C petroleum ether). A sample was submitted to chiral column analytical HPLC analysis (*iso*-hexane/*iso*-propanol = 95/5, 1 mL/min, 3.97 min (first peak), 5.14 min (second peak), 97% ee; Chiralpak AD). Optically active

2-[2H]-*tert*-butyl-1-(2-*tert*-butoxyphenyl)-3-(pentafluorophenyl)aziridine-2-carboxylate (**26**) was afforded as a yellow oil in an 82% yield.

^{1}H NMR ($CDCl_3$, 400 MHz): δ 7.09–6.83 (m, 4H, ArH), 3.30 (s, 1H, HC_3), 1.40 (s, 9H, $C(CH_3)_3$), 1.38 (s, 9H, $C(CH_3)_3$); ^{13}C NMR ($CDCl_3$, 100 MHz): 167.2, 148.2, 147.7, 147.7, 147.5, 145.3, 144,5, 144.3, 139.3, 139.1, 139.0, 136.0, 135.8, 135.8, 123.7, 123.1, 122.8, 120.7, 110.5, 110.2, 110.2, 82.1, 80.5, 43.55, 36.8, 28.6, 27.6 ppm; $[\alpha]_D^{23}$ −121 (c 1.1 $CHCl_3$); FT-IR (thin film cm^{-1}): 2979, 2933, 1743, 1738, 1594, 1524, 1502, 1451, 1393, 1369, 1331 cm^{-1}; MS (ES): 459.2 $[M+H]^+$, 481.1 $[M+Na]^+$; HRMS (EI): exact mass calculated for $[C_{23}H_{24}F_5DNO_3]$ requires 459.1812, found 459.1809.

Representative Synthesis of α-Deuterated α-Amino acid: 76

$Pd(OH)_2$/C (20% Pd by weight [9.6 mg, 0.014 mmol, 20%]) was added to a solution of optically active [2H]C_2-**16** (25 mg, 0.06 mmol) in 4 mL of ethyl acetate. The reaction mixture was stirred at 30°C under 43 psi of H_2 for 8 hr in a Biotage Endeavour catalyst screening system. The reaction was monitored by the uptake of hydrogen gas. When deemed complete, the reaction mixture was filtered through Celite and eluted with DCM. The washings were combined, and the solvent was removed under reduced pressure. The resulting material was purified by flash chromatography (15% diethyl ether in 40°C–60°C petroleum ether), allowing subsequent analysis to confirm that **76** had formed in a 64% yield. A sample was submitted to chiral column analytical HPLC analysis (*iso*-hexane/*iso*-propanol = 95/5, 1 mL/min, 4.19 min [first peak], 8.01 min [second peak], 97% ee; Chiralpak AD).

^{1}H NMR ($CDCl_3$, 300 MHz): δ 8.73 (d, 1H, *J* 4.67 Hz, Ar-H), 8.02–7.60 (m, 1H, Ar-H), 7.57–7.32 (m, 2H, Ar-H), 6.77–6.49 (m, 2H, Ar-H), 3.40 (s, 2H, β-CH_2), 1.37 (s, 9H, $C(CH_3)_3$), 1.34 (s, 9H, $C(CH_3)_3$); ^{13}C NMR ($CDCl_3$, 75 MHz): 171.6, 143.1, 141.1, 139.6, 125.7, 123.9, 123.0, 122.3, 117.2, 111.2, 82.3, 80.0, 39.1, 29.1, 28.0 ppm; $[\alpha]_D^{21}$ + 22 (c 0.5 $CHCl_3$); FT-IR (thin film): 2978, 2931, 1735, 1598, 1511, 1507, 1368, 1253, 1157 cm^{-1}; MS (EI)$^+$: *m/z* 372.3 $[M+H]^+$, 394.2 $[M+Na]^+$; HRMS (EI)$^+$: exact mass calculated for $[C_{22}H_{30}DN_2O_3]^+$ requires *m/z* 372.2392, found *m/z* 372.2396.

ACCESSION NUMBERS

cis-**27** has been deposited in the Cambridge Crystallographic Data Centre under accession number CCDC: 1510574.

SUPPLEMENTAL INFORMATION

Supplemental Information includes Supplemental Experimental Procedures and 126 figures and can be found with this article online at http://dx.doi.org/10.1016/j.chempr.2016.11.008.

AUTHOR CONTRIBUTIONS

S.P.B. designed the experiments and wrote the paper. D.U.B., G.D.H.-G., P.P., Z.D., and S.M.T. designed and conducted the experiments. M.P. and S.J.C collected and interpreted the X-ray crystal diffraction data.

ACKNOWLEDGMENTS

We gratefully acknowledge financial support from the Engineering and Physical Sciences Research Council (EPSRC) and GSK (CASE Award) (grant R13622), the University of East Anglia, the EPSRC Mass Spectroscopy Service at the University of

Wales, Swansea, and the National Crystallography Service at the University of Southampton.

Received: August 23, 2016
Revised: October 17, 2016
Accepted: November 16, 2016
Published: December 8, 2016

REFERENCES AND NOTES

1. Maltais, F., Jung, Y.C., Chen, M., Tanoury, J., Perni, R.B., Mani, N., Laitinen, L., Huang, H., Liao, S., Gao, H., et al. (2009). In vitro and in vivo isotope effects with hepatitis C protease inhibitors: enhanced plasma exposure of deuterated telaprevir versus telaprevir in rats. J. Med. Chem. *52*, 7993–8001.

2. Najjar, S.E., Blake, M.I., Benoit, P.A., and Lu, M.C. (1978). Effects of deuteration on locomotor activity of amphetamine. J. Med. Chem. *21*, 555–558.

3. Davidova, I.A., Gieg, L.M., Nanny, M., Kropp, K.G., and Suflita, J.M. (2005). Stable isotopic studies of n-alkane metabolism by a sulfate-reducing bacterial enrichment culture. Appl. Environ. Microbiol. *71*, 8174–8182.

4. Guo, C., Godoy-Ruiz, R., and Tugarinov, V. (2010). High resolution measurement of methyl 13C(m)-13C and 1H(m)-13C(m) residual dipolar couplings in large proteins. J. Am. Chem. Soc. *132*, 13984–13987.

5. Cleland, W.W. (2005). The use of isotope effects to determine enzyme mechanisms. Arch. Biochem. Biophys. *433*, 2–12.

6. Rattray, N.J.W., Hamrang, Z., Trivedi, D.K., Goodacre, R., and Fowler, S.J. (2014). Taking your breath away: metabolomics breathes life in to personalized medicine. Trends Biotechnol. *32*, 538–548.

7. Opdam, F.L., Modak, A.S., Gelderblom, H., and Guchelaar, H.J. (2015). Further characterization of a ^{13}C-dextromethorphan breath test for CYP2D6 phenotyping in breast cancer patients on tamoxifen therapy. J. Breath Res. *9*, 026003.

8. Ueki, R., Yamaguchi, K., Nonaka, H., and Sando, S. (2012). ^{1}H NMR probe for in situ monitoring of dopamine metabolism and its application to inhibitor screening. J. Am. Chem. Soc. *134*, 12398–12401.

9. Doura, T., Hata, R., Nonaka, H., Ichikawa, K., and Sando, S. (2012). Design of a ^{13}C magnetic resonance probe using a deuterated methoxy group as a long-lived hyperpolarization unit. Angew. Chem. Int. Ed. Engl. *51*, 10114–10117.

10. Kainosho, M., Torizawa, T., Iwashita, Y., Terauchi, T., Mei Ono, A., and Güntert, P. (2006). Optimal isotope labelling for NMR protein structure determinations. Nature *440*, 52–57.

11. Chan, J., Lewis, A.R., Gilbert, M., Karwaski, M.-F., and Bennet, A.J. (2010). A direct NMR method for the measurement of competitive kinetic isotope effects. Nat. Chem. Biol. *6*, 405–407.

12. Shen, Y., Xu, F., Wei, L., Hu, F., and Min, W. (2014). Live-cell quantitative imaging of proteome degradation by stimulated Raman scattering. Angew. Chem. Int. Ed. Engl. *53*, 5596–5599.

13. Fu, D., Yu, Y., Folick, A., Currie, E., Farese, R.V., Jr., Tsai, T.-H., Xie, X.S., and Wang, M.C. (2014). In vivo metabolic fingerprinting of neutral lipids with hyperspectral stimulated Raman scattering microscopy. J. Am. Chem. Soc. *136*, 8820–8828.

14. Wei, L., Yu, Y., Shen, Y., Wang, M.C., and Min, W. (2013). Vibrational imaging of newly synthesized proteins in live cells by stimulated Raman scattering microscopy. Proc. Natl. Acad. Sci. USA *110*, 11226–11231.

15. Jager, F., Ujj, L., Atkinson, G.H., and Sheves, L.N. (1996). Vibrational spectrum of K-590 containing ^{13}C14,15 retinal: Picosecond time-resolved coherent anti-stokes raman spectroscopy of the room temperature bacteriorhodopsin photocycle. J. Phys. Chem. *100*, 12066–12075.

16. Middleton, C.T., Marek, P., Cao, P., Chiu, C.-C., Singh, S., Woys, A.M., de Pablo, J.J., Raleigh, D.P., and Zanni, M.T. (2012). Two-dimensional infrared spectroscopy reveals the complex behaviour of an amyloid fibril inhibitor. Nat. Chem. *4*, 355–360.

17. Saka, S.K., Vogts, A., Kröhnert, K., Hillion, F., Rizzoli, S.O., and Wessels, J.T. (2014). Correlated optical and isotopic nanoscopy. Nat. Commun. *5*, 3664.

18. Zhang, D.-S., Piazza, V., Perrin, B.J., Rzadzinska, A.K., Poczatek, J.C., Wang, M., Prosser, H.M., Ervasti, J.M., Corey, D.P., and Lechene, C.P. (2012). Multi-isotope imaging mass spectrometry reveals slow protein turnover in hair-cell stereocilia. Nature *481*, 520–524.

19. Curran, T.G., Zhang, Y., Ma, D.J., Sarkaria, J.N., and White, F.M. (2015). MARQUIS: a multiplex method for absolute quantification of peptides and posttranslational modifications. Nat. Commun. *6*, 5924.

20. Yamada, H., Mizusawa, K., Igarashi, R., Tochio, H., Shirakawa, M., Tabata, Y., Kimura, Y., Kondo, T., Aoyama, Y., and Sando, S. (2012). Substrate/Product-targeted NMR monitoring of pyrimidine catabolism and its inhibition by a clinical drug. ACS Chem. Biol. *7*, 535–542.

21. Streitweiser, A. (2015). Hydrogen isotopes in physical organic chemistry. In Foundations of physical organic chemistry: Fifty years of the James Flack Norris AwardE.T. Strom and V.V. Mainz, eds. (American Chemical Society), pp. 77–92.

22. Higashi, T., and Ogawa, S. (2016). Isotope-coded ESI-enhancing derivatization reagents for differential analysis, quantification and profiling of metabolites in biological samples by LC/MS: A review. J. Pharm. Biomed. Anal. *130*, 181–193.

23. Shaikh, I.R. (2014). Organocatalysis: Key trends in green synthetic chemistry, challenges, scope towards heterogenization, and importance from research and industrial point of view. Journal of Catalysis *2014*, 402860.

24. Busacca, C.A., Fandrick, D.R., Song, J.J., and Senanayake, C.H. (2012). Transition Metal Catalysis in the Pharmaceutical Industry. In Applications of Transition Metal Catalysis in Drug Discovery and Development: An Industrial Perspective, M.L. Crawley and B.M. Trost, eds. (John Wiley & Sons), pp. 1–24.

25. Atzrodt, J., Derdau, V., Kerr, W.J., Reid, M., Rojahn, P., and Weck, R. (2015). Expanded applicability of iridium(I) NHC/phosphine catalysts in hydrogen isotope exchange processes with pharmaceutically-relevant heterocycles. Tetrahedron *71*, 1924–1929.

26. Lapidot, A., and Kahana, Z.E. (1986). Biological process for preparing compounds labelled with stable isotopes. Trends Biotechnol. *4*, 2–4.

27. Wohlgemuth, R. (2009). Tools and ingredients for the biocatalytic synthesis of metabolites. Biotechnol. J. *4*, 1253–1265.

28. Zhu, Y., Malerich, J.P., and Rawal, V.H. (2010). Squaramide-catalyzed enantioselective Michael addition of diphenyl phosphite to nitroalkenes. Angew. Chem. Int. Ed. Engl. *49*, 153–156.

29. Cahard, D., Xu, X., Couve-Bonnaire, S., and Pannecoucke, X. (2010). Fluorine & chirality: how to create a nonracemic stereogenic carbon-fluorine centre? Chem. Soc. Rev. *39*, 558–568.

30. Condie, A.G., González-Gómez, J.C., and Stephenson, C.R.J. (2010). Visible-light photoredox catalysis: aza-Henry reactions via C-H functionalization. J. Am. Chem. Soc. *132*, 1464–1465.

31. Müller, S., and List, B. (2009). A catalytic asymmetric 6 π electrocyclization: enantioselective synthesis of 2-pyrazolines. Angew. Chem. Int. Ed. Engl. *48*, 9975–9978.

32. Nagib, D.A., Scott, M.E., and MacMillan, D.W.C. (2009). Enantioselective

α-trifluoromethylation of aldehydes via photoredox organocatalysis. J. Am. Chem. Soc. *131*, 10875–10877.

33. Satoh, T., Sato, T., Oohara, T., and Yamakawa, K. (1989). α,β-Epoxy sulfoxides as useful intermediates in organic synthesis. 22. Stereospecific desulfinylation of sulfinylaziridines with alkylmetals: a novel synthesis including asymmetric synthesis of (Z)-N-arylaziridines and some mechanistic studies. J. Org. Chem. *54*, 3973–3978.

34. Luisi, R., Capriati, V., Florio, S., and Musio, B. (2007). Regio- and stereoselective lithiation and electrophilic substitution reactions of N-Alkyl-2,3-diphenylaziridines: solvent effect. Org. Lett. *9*, 1263–1266.

35. Vitis, L.D., Florio, L.D.S., Granito, C., Ronzini, L., Troisi, L., Capriati, V., Luisi, R., and Pilati, T. (2004). Stereoselective synthesis of heterosubstituted aziridines and their functionalization. Tetrahedron *60*, 1175–1182.

36. Troisi, L., Granito, C., Carlucci, C., Bona, F., and Florio, S. (2006). Synthesis and functionalisation of 2,3-diheterocycle-substituted aziridines. Eur. J. Org. Chem. 775–781.

37. Müller, P., Riegert, D., and Bernardinelli, G. (2004). Desymmetrization of N-sulfonated aziridines by alkyllithium reagents in the presence of chiral ligands. Helv. Chim. Acta *87*, 227–239.

38. Lowpetch, K., and Young, D.W. (2005). A short, versatile chemical synthesis of L- and D-amino acids stereoselectively labelled solely in the beta position. Org. Biomol. Chem. *3*, 3348–3356.

39. Axelsson, B.S., O' Toole, K.J., Spencer, P.A., and Young, D.W. (1994). Versatile synthesis of stereospecifically labelled D-amino acids via labelled aziridines - preparation of (2R,3S)-[3-$^{2}H_1$]- and (2R,3R)-[2,3-$^{2}H_2$]-serine; (2S,2′S,3S,3′S)-[3,3′-$^{2}H_2$]- and (2S,2′S,3R,3′R)-[2,2′,3,3′-$^{2}H_4$]-cystine; and (2S,3S)-[3-$^{2}H_1$-] and (2S,3R)-[2,3-$^{2}H_2$]-β-chloroalanine. J. Chem. Soc. Perkin *1*, 807–815.

40. Satoh, T., and Kukuda, Y. (2003). A new synthesis of enantiomerically pure α- and β-amino acid derivatives using aziridinyl anions. Tetrahedron *59*, 9803–9810.

41. Affortunato, F., Florio, S., Luisi, R., and Musio, B. (2008). α- vs ortho-lithiation of N-alkylarylaziridines: probing the role of the nitrogen inversion process. J. Org. Chem. *73*, 9214–9220.

42. Concellón, J.M., Suárez, J.R., García-Granda, S., and Rosario, D.M. (2004). Synthesis and stereoselective lithiation of enantiopure 2-(1-aminoalkyl)aziridine–borane complexes. Angew. Chem. Int. Ed. Engl. *43*, 4333–4336.

43. Wenkert, D., Ferguson, S.B., Porter, B., and Qvarnstrom, A. (1985). Thermal transformation of alkenoylated aziridines into ring-fused pyrrolidines. J. Org. Chem. *50*, 4114–4119.

44. Ochiai, M., and Kitagawa, Y. (1999). Aziridination of activated imines with monocarbonyl iodonium ylides generated from (Z)-(2-acetoxyvinyl)iodonium salts via ester exchange:cstereoselective synthesis of 2-acylaziridines. J. Org. Chem. *64*, 3181–3189.

45. Nagel, D.L., Woller, P.B., and Cromwell, N.H. (1971). Nuclear magnetic resonance spectra and nitrogen inversion in 1-alkyl-2-aryl-3-carboaziridines. J. Org. Chem. *36*, 3911–3917.

46. Padwa, A., and Eisenhardt, W. (1975). Photochemical transformations of small-ring carbonyl compounds. XXVIII. 1,5-Hydrogen transfer in the photochemistry of aroylaziridines. J. Am. Chem. Soc. *93*, 1400–1408.

47. Woller, P.B., and Chromwell, N.H. (1970). 1,3-Dipolar cycloaddition reactions of the geometrical isomers of some methyl 1-alkyl-2-(p-biphenylyl)-3-aziridinecarboxylates. J. Org. Chem. *35*, 888–898.

48. Capriati, V., Florio, S., Luisi, R., and Musio, B. (2005). Directed ortho lithiation of N-alkylphenylaziridines. Org. Lett. *7*, 3749–3752.

49. Satoh, T., Ozawa, M., Takano, K., Chyouma, T., and Okawa, A. (2000). Generation of aziridinyllithiums from sulfinylaziridines with tert-butyllithium: properties, reactivity, and application to a synthesis of α,α-dialkylamino acid esters and amides including an optically active form. Tetrahedron *56*, 4415–4425.

50. Moody, C.J., and Hughes, R.A. (2007). From amino acids to heteroaromatics - Thiopeptide antibiotics, Natures heterocyclic peptides. Angew. Chem. Int. Ed. Engl. *46*, 7930–7954.

51. Sengupta, I., Nadaud, P.S., Helmus, J.J., Schwieters, C.D., and Jaroniec, C.P. (2012). Protein fold determined by paramagnetic magic-angle spinning solid-state NMR spectroscopy. Nat. Chem. *4*, 410–417.

52. Lange, A., Luca, S., and Baldus, M. (2002). Structural constraints from proton-mediated rare-spin correlation spectroscopy in rotating solids. J. Am. Chem. Soc. *124*, 9704–9705.

53. Jaroniec, C.P., Filip, C., and Griffin, R.G. (2002). 3D TEDOR NMR experiments for the simultaneous measurement of multiple carbon-nitrogen distances in uniformly ^{13}C, ^{15}N-labeled solids. J. Am. Chem. Soc. *124*, 10728–10742.

54. Franks, W.T., Wylie, B.J., Stellfox, S.A., and Rienstra, C.M. (2006). Backbone conformational constraints in a microcrystalline U-^{15}N-labeled protein by 3D dipolar-shift solid-state NMR spectroscopy. J. Am. Chem. Soc. *128*, 3154–3155.

55. Wang, T.J., Larson, M.G., Vasan, R.S., Cheng, S., Rhee, E.P., McCabe, E., Lewis, G.D., Fox, C.S., Jacques, P.F., Fernandez, C., et al. (2011). Metabolite profiles and the risk of developing diabetes. Nat. Med. *17*, 448–453.

56. Zhang, Q., Li, Y., Chen, D., Yu, Y., Duan, L., Shen, B., and Liu, W. (2011). Radical-mediated enzymatic carbon chain fragmentation-recombination. Nat. Chem. Biol. *7*, 154–160.

57. Ramazzina, I., Costa, R., Cendron, L., Berni, R., Peracchi, A., Zanotti, G., and Percudani, R. (2010). An aminotransferase branch point connects purine catabolism to amino acid recycling. Nat. Chem. Biol. *6*, 801–806.

58. Mann, M. (2006). Functional and quantitative proteomics using SILAC. Nat. Rev. Mol. Cell Biol. *7*, 952–958.

59. Adibekian, A., Martin, B.R., Wang, C., Hsu, K.-L., Bachovchin, D.A., Niessen, S., Hoover, H., and Cravatt, B.F. (2011). Click-generated triazole ureas as ultrapotent in vivo-active serine hydrolase inhibitors. Nat. Chem. Biol. *7*, 469–478.

60. Hanash, S., and Taguchi, A. (2010). The grand challenge to decipher the cancer proteome. Nat. Rev. Cancer *10*, 652–660.

61. Willmann, J.K., van Bruggen, N., Dinkelborg, L.M., and Gambhir, S.S. (2008). Molecular imaging in drug development. Nat. Rev. Drug Discov. *7*, 591–607.

62. Watts, A. (2005). Solid-state NMR in drug design and discovery for membrane-embedded targets. Nat. Rev. Drug Discov. *4*, 555–568.

63. Lappin, G., and Garner, R.C. (2003). Big physics, small doses: the use of AMS and PET in human microdosing of development drugs. Nat. Rev. Drug Discov. *2*, 233–240.

64. Wood, K., Lehnert, U., Kessler, B., Zaccai, G., and Oesterhelt, D. (2008). Hydration dependence of active core fluctuations in bacteriorhodopsin. Biophys. J. *95*, 194–202.

65. Réat, V., Patzelt, H., Ferrand, M., Pfister, C., Oesterhelt, D., and Zaccai, G. (1998). Dynamics of different functional parts of bacteriorhodopsin: H-^{2}H labeling and neutron scattering. Proc. Natl. Acad. Sci. USA *95*, 4970–4975.

66. Stegmann, R., Manakova, E., Rössle, M., Heumann, H., Nieba-Axmann, S.E., Plückthun, A., Hermann, T., May, R.P., and Wiedenmann, A. (1998). Structural changes of the Escherichia coli GroEL-GroES chaperonins upon complex formation in solution: a neutron small angle scattering study. J. Struct. Biol. *121*, 30–40.

67. Gygi, S.P., Rist, B., Gerber, S.A., Turecek, F., Gelb, M.H., and Aebersold, R. (1999). Quantitative analysis of complex protein mixtures using isotope-coded affinity tags. Nat. Biotechnol. *17*, 994–999.

68. Han, D.K., Eng, J., Zhou, H., and Aebersold, R. (2001). Quantitative profiling of differentiation-induced microsomal proteins using isotope-coded affinity tags and mass spectrometry. Nat. Biotechnol. *19*, 946–951.

69. Castro-Gamero, A.M., Izumi, C., and Rosa, J.C. (2014). Biomarker verification using selected reaction monitoring and shotgun proteomics. Methods Mol. Biol. *1156*, 295–306.

70. Kriwacki, R.W., Wu, J., Siuzdak, G., and Wright, P.E. (1996). Probing protein/protein interactions with mass spectrometry and isotopic labeling: analysis of the p21/Cdk2 complex. J. Am. Chem. Soc. *118*, 5320–5321.

71. Wang, Y., Filippov, I., Richter, C., Luo, R., and Kriwacki, R.W. (2005). Solution NMR studies of an intrinsically unstructured protein within a dilute, 75 kDa eukaryotic protein assembly; probing the practical limits for efficiently assigning polypeptide backbone resonances. ChemBioChem *6*, 2242–2246.

72. Hajduk, P.J., Mack, J.C., Olejniczak, E.T., Park, C., Dandliker, P.J., and Beutel, B.A. (2004). SOS-NMR: a saturation transfer NMR-based

method for determining the structures of protein-ligand complexes. J. Am. Chem. Soc. *126*, 2390–2398.

73. Zhu, J., and Bienaymé, H., eds. (2005). Multicomponent Reactions (Wiley-VCH).

74. Yu, J., Shi, F., and Gong, L.-Z. (2011). Brønsted-acid-catalyzed asymmetric multicomponent reactions for the facile synthesis of highly enantioenriched structurally diverse nitrogenous heterocycles. Acc. Chem. Res. *44*, 1156–1171.

75. Ly, F., Liu, S., and Hu, W. (2013). Recent advances in the use of chiral Brønsted acids as cooperative catalysts in cascade and multicomponent reactions. Asian J. Org. Chem. *2*, 824–836.

76. Knowles, R.R., and Jacobsen, E.N. (2010). Attractive noncovalent interactions in asymmetric catalysis: links between enzymes and small molecule catalysts. Proc. Natl. Acad. Sci. USA *107*, 20678–20685.

77. Joyce, L.A., Shabbir, S.H., and Anslyn, E.V. (2010). The uses of supramolecular chemistry in synthetic methodology development: examples of anion and neutral molecular recognition. Chem. Soc. Rev. *39*, 3621–3632.

78. Sparr, C., and Gilmour, R. (2010). Fluoro-organocatalysts: conformer equivalents as a tool for mechanistic studies. Angew. Chem. Int. Ed. Engl. *49*, 6520–6523.

79. Devery, J.J., 3rd, Conrad, J.C., MacMillan, D.W.C., and Flowers, R.A., 2nd (2010). Mechanistic complexity in organo-SOMO activation. Angew. Chem. Int. Ed. Engl. *49*, 6106–6110.

80. Yoon, T.P., Ischay, M.A., and Du, J. (2010). Visible light photocatalysis as a greener approach to photochemical synthesis. Nat. Chem. *2*, 527–532.

81. Alba, A.N.R., Companyó, X., and Rios, R. (2010). Sulfones: new reagents in organocatalysis. Chem. Soc. Rev. *39*, 2018–2033.

82. List, B. (2010). Emil Knoevenagel and the roots of aminocatalysis. Angew. Chem. Int. Ed. Engl. *49*, 1730–1734.

83. Grondal, C., Jeanty, M., and Enders, D. (2010). Organocatalytic cascade reactions as a new tool in total synthesis. Nat. Chem. *2*, 167–178.

84. Jiang, H., Paixão, M.W., Monge, D., and Jørgensen, K.A. (2010). Acyl phosphonates: good hydrogen bond acceptors and ester/amide equivalents in asymmetric organocatalysis. J. Am. Chem. Soc. *132*, 2775–2783.

85. Kamioka, S., Ajami, D., and Rebek, J., Jr. (2010). Autocatalysis and organocatalysis with synthetic structures. Proc. Natl. Acad. Sci. USA *107*, 541–544.

86. Fu, X., Loh, W.T., Zhang, Y., Chen, T., Ma, T., Liu, H., Wang, J., and Tan, C.-H. (2009). Chiral guanidinium salt catalyzed enantioselective phospha-Mannich reactions. Angew. Chem. Int. Ed. Engl. *48*, 7387–7390.

87. Pinacho Crisóstomo, F.R., Lledó, A., Shenoy, S.R., Iwasawa, T., and Rebek, J., Jr. (2009). Recognition and organocatalysis with a synthetic cavitand receptor. J. Am. Chem. Soc. *131*, 7402–7410.

88. Lu, L.Q., Cao, Y.J., Liu, X.P., An, J., Yao, C.J., Ming, Z.H., and Xiao, W.J. (2008). A new entry to cascade organocatalysis: reactions of stable sulfur ylides and nitroolefins sequentially catalyzed by thiourea and DMAP. J. Am. Chem. Soc. *130*, 6946–6948.

89. Barbas, C.F., 3rd (2008). Organocatalysis lost: modern chemistry, ancient chemistry, and an unseen biosynthetic apparatus. Angew. Chem. Int. Ed. Engl. *47*, 42–47.

90. Bertelsen, S., Nielsen, M., and Jørgensen, K.A. (2007). Radicals in asymmetric organocatalysis. Angew. Chem. Int. Ed. Engl. *46*, 7356–7359.

91. Carlone, A., Cabrera, S., Marigo, M., and Jørgensen, K.A. (2007). A new approach for an organocatalytic multicomponent domino asymmetric reaction. Angew. Chem. Int. Ed. Engl. *46*, 1101–1104.

92. Desai, A.A., and Wulff, W.D. (2010). Controlled diastereo- and enantioselection in a catalytic asymmetric aziridination. J. Am. Chem. Soc. *132*, 13100–13103.

93. Hashimoto, T., Nakatsu, H., Watanabe, S., and Maruoka, K. (2010). Stereoselective synthesis of trisubstituted aziridines with N-α-diazoacyl camphorsultam. Org. Lett. *12*, 1668–1671.

94. Zeng, X., Zeng, X., Xu, Z., Lu, M., and Zhong, G. (2009). Highly efficient asymmetric trans-selective aziridination of diazoacetamides and N-Boc-imines catalyzed by chiral Brønsted acids. Org. Lett. *11*, 3036–3039.

95. Rowland, E.B., Rowland, G.B., Rivera-Otero, E., and Antilla, J.C. (2007). Brønsted acid-catalyzed desymmetrization of meso-aziridines. J. Am. Chem. Soc. *129*, 12084–12085.

96. Mahoney, J.M., Smith, C.R., and Johnston, J.N. (2005). Bronsted acid-promoted olefin aziridination and formal anti-aminohydroxylation. J. Am. Chem. Soc. *127*, 1354–1355.

97. Williams, A.L., and Johnston, J.N. (2004). The Brønsted acid-catalyzed direct aza-Darzens synthesis of N-alkyl cis-aziridines. J. Am. Chem. Soc. *126*, 1612–1613.

98. Bew, S.P., Ashford, P.-A., and Bachera, D.U. (2013). Synthesis of structure and function diverse α-D-diazoacetates, α-D-diazoacetamides, α-D-diazoketones and the antibiotic α-D-azaserine. Synthesis *15*, 3805–3807.

99. Despotović, I., Kovacević, B., and Maksić, Z.B. (2007). Derivatives of azacalix[3](2,6)pyridine are strong neutral organic superbases: a DFT study. Org. Lett. *9*, 1101–1104.

100. Bell, T.W., Choi, H.-J., Harte, W., and Drew, M.G.B. (2003). Syntheses, conformations, and basicities of bicyclic triamines. J. Am. Chem. Soc. *125*, 12196–12210.

101. Lan, T., and McLaughlin, L.W. (2001). The energetic contribution of a bifurcated hydrogen bond to the binding of DAPI to dA-dT rich sequences of DNA. J. Am. Chem. Soc. *123*, 2064–2065.

102. Tworowska, I., and Nikonowicz, E.P. (2006). Base pairing within the ψ32,ψ39-modified anticodon arm of Escherichia coli tRNA(Phe). J. Am. Chem. Soc. *128*, 15570–15571.

103. Yamanaka, M., Itoh, J., Fuchibe, K., and Akiyama, T. (2007). Chiral Brønsted acid catalyzed enantioselective Mannich-type reaction. J. Am. Chem. Soc. *129*, 6756–6764.

104. Parmar, D., Sugiono, E., Raja, S., and Rueping, M. (2014). Complete field guide to asymmetric BINOL-phosphate derived Brønsted acid and metal catalysis: history and classification by mode of activation; Brønsted acidity, hydrogen bonding, ion pairing, and metal phosphates. Chem. Rev. *114*, 9047–9153.

105. Nakashima, D., and Yamamoto, H. (2006). Design of chiral N-triflyl phosphoramide as a strong chiral Brønsted acid and its application to asymmetric Diels-Alder reaction. J. Am. Chem. Soc. *128*, 9626–9627.

106. Rueping, M., Ieawsuwan, W., Antonchick, A.P., and Nachtsheim, B.J. (2007). Chiral Brønsted acids in the catalytic asymmetric Nazarov cyclization–the first enantioselective organocatalytic electrocyclic reaction. Angew. Chem. Int. Ed. Engl. *46*, 2097–2100.

107. Rueping, M., Nachtsheim, B.J., Moreth, S.A., and Bolte, M. (2008). Asymmetric Brønsted acid catalysis: enantioselective nucleophilic substitutions and 1,4-additions. Angew. Chem. Int. Ed. Engl. *47*, 593–596.

108. Cheon, C.H., and Yamamoto, H. (2008). A Brønsted acid catalyst for the enantioselective protonation reaction. J. Am. Chem. Soc. *130*, 9246–9247.

109. Enders, D., Narine, A.A., Toulgoat, F., and Bisschops, T. (2008). Asymmetric Brønsted acid catalyzed isoindoline synthesis: enhancement of enantiomeric ratio by stereoablative kinetic resolution. Angew. Chem. Int. Ed. Engl. *47*, 5661–5665.

110. Rueping, M., Theissmann, T., Kuenkel, A., and Koenigs, R.M. (2008). Highly enantioselective organocatalytic carbonyl-ene reaction with strongly acidic, chiral Brønsted acids as efficient catalysts. Angew. Chem. Int. Ed. Engl. *47*, 6798–6801.

111. Zeng, M., Kang, Q., He, Q.-L., and You, S.-L. (2008). Highly enantioselective Friedel-Crafts reaction of 4,7-dihydroindoles with β,γ-unsaturated α-keto esters by chiral Brønsted acids. Adv. Syn. Cat. *350*, 2169–2173.

112. Rueping, M., and Leawsuwan, W. (2009). A Catalytic asymmetric electrocyclization-protonation Reaction. Adv. Syn. Cat. *351*, 78–84.

113. Patureau, F.W., de Boer, S., Kuil, M., Meeuwissen, J., Breuil, P.-A.R., Siegler, M.A., Spek, A.L., Sandee, A.J., de Bruin, B., and Reek, J.N.H. (2009). Sulfonamido-phosphoramidite ligands in cooperative dinuclear hydrogenation catalysis. J. Am. Chem. Soc. *131*, 6683–6685.

114. Yue, T., Wang, M.-X., Wang, D.-X., Masson, G., and Zhu, J. (2009). Brønsted acid catalyzed enantioselective three-component reaction involving the α addition of isocyanides to imines. Angew. Chem. Int. Ed. Engl. *48*, 6717–6721.

115. Rueping, M., and Lin, M.-Y. (2010). Catalytic asymmetric mannich-ketalization reaction: highly enantioselective synthesis of aminobenzopyrans. Chemistry *16*, 4169–4172.

116. Cheon, C.H., and Yamamoto, H. (2010). N-triflylthiophosphoramide catalyzed enantioselective Mukaiyama aldol reaction of aldehydes with silyl enol ethers of ketones. Org. Lett. *12*, 2476–2479.

117. Gutierrez, E.G., Moorhead, E.J., Smith, E.H., Lin, V., Ackerman, L.K.G., Knezevic, C.E., Sun, V., Grant, S., and Wenzel, A.G. (2010). Electron-withdrawing, biphenyl-2,2′-diol-based compounds for asymmetric catalysis. Eur. J. Org. Chem. 3027–3031.

118. Wakchaure, V.N., and List, B. (2010). A new structural motif for bifunctional Brønsted acid/base organocatalysis. Angew. Chem. Int. Ed. Engl. *49*, 4136–4139.

119. Enders, D., Seppelt, M., and Beck, T. (2010). Enantioselective organocatalytic synthesis of arylglycines via Friedel–Crafts alkylation of arenes with a glyoxylate imine. Adv. Syn. Cat. *352*, 1413–1418.

120. Bew, S.P., Carrington, R., Hughes, D.L., Liddle, J., and Pesce, P. (2009). An organocatalytic synthesis of cis-N-alkyl- and N-arylaziridine carboxylates. Adv. Syn. Cat. *351*, 2579–2588.

121. Barnett, D.W., Panigot, M.J., and Curley, R.W. (2002). Stereoselective route to ^{15}N-labeled-β-deuterated amino acids: synthesis of (2S,3R)-[3-^{2}H,^{15}N]-phenylalanine. Tetrahedron Asymmetry *13*, 1893–1900.

122. Maitra, U., and Chandrasekhar, J. (1997). Use of isotopes for studying reaction mechanisms: Secondary kinetic isotope effect. Resonance *2*, 18–25.

123. A satisfactory explanation that accounts for this observation has yet to be established; however, steric and/or electronic factors seem important. DFT studies towards understanding the mechanism will be reported in due course.

124. Hashimoto, T., Uchiyama, N., and Maruoka, K. (2008). Trans-selective asymmetric aziridination of diazoacetamides and N-Boc imines catalyzed by axially chiral dicarboxylic acid. J. Am. Chem. Soc. *130*, 14380–14381.

125. Reid, J.P., Simón, L., and Goodman, J.M.A. (2016). A practical guide for predicting the stereochemistry of bifunctional phosphoric acid catalyzed reactions of Imines. Acc. Chem. Res. *49*, 1029–1041.

126. Sai, M., and Yamamoto, H. (2015). Chiral Brønsted acid as a true catalyst: asymmetric mukaiyama aldol and hosomi-sakurai allylation reactions. J. Am. Chem. Soc. *137*, 7091–7094.

127. Davies, S.G., Rodriguez-Solla, H., Tamayo, J.A., Cowley, A.R., Concellon, C., Garner, A.C., Parkes, A.L., and Smith, A.D. (2005). Asymmetric conjugate reductions with samarium diiodide: asymmetric synthesis of (2S,3R)- and (2S,3S)-[2-2H,3-2H]-leucine-(S)-phenylalanine dipeptides and (2S,3R)-[2-(2)H,3-2H]-phenylalanine methyl ester. Org. Biomol. Chem. *3*, 1435–1447.

128. Maegawa, T., Akashi, A., Esaki, H., Aoki, F., Sajiki, H., and Hirota, K. (2005). Efficient and selective deuteration of phenylalanine derivatives catalysed by Pd/C. Synlett, 845–847.

129. Boroda, E., Rakowska, S., Kanski, S., and Kanska, R. (2003). Enzymatic synthesis of L-tryptophan and 5-hydroxy-L-tryptophan labelled with deuterium and tritium at the α-carbon position. J. Labelled Comp. Radiopharm. *4*, 691–698.

130. Lygo, B., and Humphreys, L.D. (2002). Enantioselective synthesis of α-carbon deuterium-labelled L-α-amino acids. Tetrahedron Lett. *43*, 6677–6679.

131. Mitulovi, G., Lammerhofer, M., Maier, N.M., and Lindner, W. (2000). Simple and efficient preparation of (R)- and (S)-enantiomers of α-carbon deuterium-labelled α-amino acids. J. Labelled Comp. Radiopharm. *43*, 449–461.

132. Lim, Y.-H., Yoshimura, T., Soda, K., and Esaki, N. (1998). Stereospecific labeling at α-position of phenylalanine and phenylglycine with amino acid racemase. J. Ferment. Bioeng. *86*, 400–402.

133. Oba, M., Terauchi, T., Owari, Y., Imai, Y., Motoyama, I., and Nishiyama, K. (1998). Stereodivergent synthesis of L-threo- and L-erythro-[2,3-^{2}H2] amino acids using optically active dioxopiperazine as a chiral template. J. Chem. Soc., Perkin Trans. 1, 1275–1282.

134. Kelly, N.M., Sutherland, A., and Willis, C.L. (1997). Synthesis of amino acids incorporating stable isotopes. Nat. Prod. Rep. *14*, 205–219.

135. Elemes, Y., and Ragnarsson, U. (1996). Synthesis of enantiopure α-deuterated Boc-L-amino acids. J. Chem. Soc., Perkin Trans. 1 *6*, 537–540.

136. Milne, J.J., and Malthouse, J.P.G. (1996). Enzymatic synthesis of α-deuterated amino acids. Biochem. Soc. Trans. *24*, 133S.

137. Rose, J.E., Leeson, P.D., and Gani, D. (1995). Stereospecific synthesis of α-deuterated α-amino acids: regiospecific deuteration of chiral 3-isopropyl-2,5-dimethoxy-3,6-dihydropyrazines. J. Chem. Soc., Perkin Trans. 1, 157–165.

138. Axelsson, B.S., O'Toole, K.J., Spencer, P.A., and Young, D.W. (1991). A versatile synthesis of stereospecificaily labelled D-amino acids and related enzyme inhibitors. Chem. Comm. 1085–1086.

139. Gelb, M.H., Lin, Y., Pickard, M.A., Song, Y., and Vederas, J.C. (1990). Synthesis of 3-fluorodiaminopimelic acid isomers as inhibitors of diaminopimelate epimerase: stereocontrolled enzymatic elimination of hydrogen fluoride. J. Am. Chem. Soc. *112*, 4932–4942.

140. Seebach, D., Dziadulewicz, E., Behrendt, L., Cantoreggi, S., and Fitzi, R. (1989). Synthesis of nonproteinogenic (R)- or (S)-amino acid analogues of phenylalanine, isotopically labelled and cyclic amino acids from tert-butyl 2-(tert-Butyl)-3-methyl-4-oxo-1-imidazolidinecarboxylate (Boc-BMI). Liebigs Ann. Chem. 1215–1232.

141. Fujihara, H., and Schowen, R.L. (1984). Facile Economical synthesis of L-[α-2H]-α-amino acids. J. Org. Chem. *49*, 2819–2820.

142. Igarashi, S., Osawa, M., Takeuchi, K., Ozawa, S., and Shimada, I. (2008). Amino acid selective cross-saturation method for identification of proximal residue pairs in a protein-protein complex. J. Am. Chem. Soc. *130*, 12168–12176.

143. Gross, H., Stockwell, V.O., Henkels, M.D., Nowak-Thompson, B., Loper, J.E., and Gerwick, W.H. (2007). The genomisotopic approach: a systematic method to isolate products of orphan biosynthetic gene clusters. Chem. Biol. *14*, 53–63.

144. Tonelli, M., Masterson, L.R., Cornilescu, G., Markley, J.L., and Veglia, G. (2009). One-sample approach to determine the relative orientations of proteins in ternary and binary complexes from residual dipolar coupling measurements. J. Am. Chem. Soc. *131*, 14138–14139.

145. Heller, M., Sukopp, M., Tsomaia, N., John, M., Mierke, D.F., Reif, B., and Kessler, H. (2006). The conformation of cyclo(-D-Pro-Ala4-) as a model for cyclic pentapeptides of the DL4 type. J. Am. Chem. Soc. *128*, 13806–13814.

146. Tamamura, H., Hiramatsu, K., Ueda, S., Wang, Z., Kusano, S., Terakubo, S., Trent, J.O., Peiper, S.C., Yamamoto, N., Nakashima, H., et al. (2005). Stereoselective synthesis of [L-Arg-L/D-3-(2-naphthyl)alanine]-type (E)-alkene dipeptide isosteres and its application to the synthesis and biological evaluation of pseudopeptide analogues of the CXCR4 antagonist FC131. J. Med. Chem. *48*, 380–391.

147. Wiegerinck, P.H.G., Hofstede, L.W.H., Sperling, F.M.G.M., and Vader, J.F. (2008). Synthesis of ^{14}C- and ^{14}C3-labelled Org 37462. J. Labelled Comp. Radiopharm. *51*, 195–201.

148. Shaginian, A., Whitby, L.R., Hong, S., Hwang, I., Farooqi, B., Searcey, M., Chen, J., Vogt, P.K., and Boger, D.L. (2009). Design, synthesis, and evaluation of an α-helix mimetic library targeting protein-protein interactions. J. Am. Chem. Soc. *131*, 5564–5572.

149. Adamczyk, M., Akireddy, S.R., and Reddy, R.E. (2001). Enantioselective synthesis of (2-pyridyl) alanines via catalytic hydrogenation and application to the synthesis of L-azatyrosine. Org. Lett. *3*, 3157–3159.

150. Huang, F., Nie, Y., Ye, F., Zhang, M., and Xia, J. (2015). Site Selective Azo Coupling for Peptide Cyclization and Affinity Labeling of an SH3 Protein. Bioconjug. Chem. *26*, 1613–1622.

151. Horowitz, S., Adhikari, U., Dirk, L.M.A., Del Rizzo, P.A., Mehl, R.A., Houtz, R.L., Al-Hashimi, H.M., Scheiner, S., and Trievel, R.C. (2014). Manipulating unconventional CH-based hydrogen bonding in a methyltransferase via noncanonical amino acid mutagenesis. ACS Chem. Biol. *9*, 1692–1697.

152. Blanden, A.R., Mukherjee, K., Dilek, O., Loew, M., and Bane, S.L. (2011). 4-aminophenylalanine as a biocompatible nucleophilic catalyst for hydrazone ligations at

low temperature and neutral pH. Bioconjug. Chem. *22*, 1954–1961.

153. Rowe, L., Ensor, M., Mehl, R., and Daunert, S. (2010). Modulating the bioluminescence emission of photoproteins by in vivo site-directed incorporation of non-natural amino acids. ACS Chem. Biol. *5*, 455–460.

154. Iijima, I., and Hohsaka, T. (2009). Position-specific incorporation of fluorescent non-natural amino acids into maltose-binding protein for detection of ligand binding by FRET and fluorescence quenching. ChemBioChem *10*, 999–1006.

155. Chang, M.C.Y., Yee, C.S., Nocera, D.G., and Stubbe, J. (2004). Site-specific replacement of a conserved tyrosine in ribonucleotide reductase with an aniline amino acid: a mechanistic probe for a redox-active tyrosine. J. Am. Chem. Soc. *126*, 16702–16703.

156. Wang, L., Xie, J., Deniz, A.A., and Schultz, P.G. (2003). Unnatural amino acid mutagenesis of green fluorescent protein. J. Org. Chem. *68*, 174–176.

157. Kraut, D.A., Churchill, M.J., Dawson, P.E., and Herschlag, D. (2009). Evaluating the potential for halogen bonding in the oxyanion hole of ketosteroid isomerase using unnatural amino acid mutagenesis. ACS Chem. Biol. *4*, 269–273.

158. Heredia, D., Natera, J., Gervaldo, M., Otero, L., Fungo, F., Lin, C.Y., and Wong, K.T. (2010). Spirobifluorene-bridged donor/acceptor dye for organic dye-sensitized solar cells. Org. Lett. *12*, 12–15.

159. Grauer, A., Späth, A., Ma, D., and König, B. (2009). Metal-catalyzed derivatization of C(α)-tetrasubstituted amino acids and their use in the synthesis of cyclic peptides. Chem. Asian J. *4*, 1134–1140.

160. Degoey, D.A., Grampovnik, D.J., Flentge, C.A., Flosi, W.J., Chen, H.J., Yeung, C.M., Randolph, J.T., Klein, L.L., Dekhtyar, T., Colletti, L., et al. (2009). 2-Pyridyl P1′-substituted symmetry-based human immunodeficiency virus protease inhibitors (A-792611 and A-790742) with potential for convenient dosing and reduced side effects. J. Med. Chem. *52*, 2571–2586.

161. Herbert, R.B., and Knaggs, A.R. (1992). Biosynthesis of the antibiotic obafluorin from D-[U-^{13}C]-glucose and p-aminophenylalanaine in Pseudomonas fluorescens. J. Chem. Soc., Perkin Trans. *1*, 103–107.

162. Matthews, H.R., Matthews, K.S., and Opella, S. (1977). Selectively deuterated amino acid analogues synthesis, Incorporation into proteins and NMR properties. Biochimica et Biophysica Acta. General Subjects *497*, 1–13.

163. Sheppard, D., Li, D.-W., Brüschweiler, R., and Tugarinov, V. (2009). Deuterium spin probes of backbone order in proteins: ^{2}H NMR relaxation study of deuterated carbon alpha sites. J. Am. Chem. Soc. *131*, 15853–15865.

164. Young, D.D., Young, T.S., Jahnz, M., Ahmad, I., Spraggon, G., and Schultz, P.G. (2011). An evolved aminoacyl-tRNA synthetase with atypical polysubstrate specificity. Biochemistry *50*, 1894–1900.

165. Yuvienco, C., More, H.T., Haghpanah, J.S., Tu, R.S., and Montclare, J.K. (2012). Modulating supramolecular assemblies and mechanical properties of engineered protein materials by fluorinated amino acids. Biomacromolecules *13*, 2273–2278.

166. Borozan, S.Z., and Stojanović, S.D. (2013). Halogen bonding in complexes of proteins and non-natural amino acids. Comput. Biol. Chem. *47*, 231–239.

167. Yang, C.Y., Renfrew, P.D., Olsen, A.J., Zhang, M., Yuvienco, C., Bonneau, R., and Montclare, J.K. (2014). Improved stability and half-life of fluorinated phosphotriesterase using rosetta. ChemBioChem *15*, 1761–1764.

168. Pott, M., Schmidt, M.J., and Summerer, D. (2014). Evolved sequence contexts for highly efficient amber suppression with noncanonical amino acids. ACS Chem. Biol. *9*, 2815–2822.

169. Liu, S., Yang, Y., Zhao, C., Huang, J., Han, C., and Han, J. (2014). Effect of the 4′-substituted phenylalanine moiety of sansalvamide A peptide on antitumor activity. J. Med. Chem. Commun. *5*, 463–467.

170. Upadhyaya, P., Qian, Z., Selner, N.G., Clippinger, S.R., Wu, Z., Briesewitz, R., and Pei, D. (2015). Inhibition of Ras signaling by blocking Ras-effector interactions with cyclic peptides. Angew. Chem. Int. Ed. Engl. *54*, 7602–7606.

171. Hsu, W.-L., Shih, T.-C., and Horng, J.-C. (2015). Folding stability modulation of the villin headpiece helical subdomain by 4-fluorophenylalanine and 4-methylphenylalanine. Biopolymers *103*, 627–637.

172. Davies, S.G., Fletcher, A.M., Frost, A.B., Lee, J.A., Roberts, P.M., and Thomson, J.E. (2013). Trading N and O: asymmetric syntheses of β-hydroxy- α-amino acids via β-hydroxy-α-amino esters. Tetrahedron *69*, 8885–8898.

173. He, Z.-T., Zhao, Y.-S., Tian, P., Wang, C.-C., Dong, H.-Q., and Lin, G.-Q. (2014). Copper-catalyzed asymmetric hydroboration of α-dehydroamino acid derivatives: facile synthesis of chiral β-hydroxy-α-amino acids. Org. Lett. *16*, 1426–1429.

174. Seebach, D., and Aebi, J.D. (1984). α-Alkylation of serine with self-reproduction of the center of chirality. Tetrahedron Lett. *25*, 2545–2548.

175. Schollkopf, U., and Beulshausen, T. (1989). Asymmetric syntheses via heterocyclic intermediates, XLII. Asymmetric syntheses of diastereomerically and enantiomerically pure (2R,3S)-threo-3-arylserine methyl esters by the bis-lactim ether method asymmetric synthesis of chloramphenicol. Liebigs Ann. Chem. *1989*, 223–225.

176. Hayashi, T., Sawamura, M., and Ito, Y. (1992). Asymmetric synthesis catalyzed by chiral ferrocenylphosphine transition metal complexes. 10 gold(I)-catalyzed asymmetric aldol reaction of isocyanoacetate. Tetrahedron *48*, 1999–2012.

177. Morán-Ramallal, R., Liz, R., and Gotor, V. (2010). Enantiopure trans-3-arylaziridine-2-carboxamides: preparation by bacterial hydrolysis and ring-openings toward enantiopure, unnatural D-α-amino acids. J. Org. Chem. *75*, 6614–6624.

178. Fan, S., Liu, S., Zhang, H., Liu, Y., Yang, Y., and Jin, L. (2014). Biocatalytic synthesis of enantiopure β-methoxy-β-arylalanine derivatives. Eur. J. Org. Chem. *25*, 5591–5597.

179. Zhao, G.-H., Li, H., Liu, W., Zhang, W.-G., Zhang, F., Liu, Q., and Jiao, Q.-C. (2011). Preparation of optically active β-hydroxy-α-amino acid by immobilized Escherichia coli cells with serine hydroxymethyl transferase activity. Amino Acids *40*, 215–220.

180. Fesko, K., Uhl, M., Steinreiber, J., Gruber, K., and Griengl, H. (2010). Biocatalytic access to α,α-dialkyl-α-amino acids by a mechanism-based approach. Angew. Chem. Int. Ed. Engl. *49*, 121–124.

181. Noyori, R., Ikeda, T., Ohkuma, T., Wldhalm, M., Kitamura, M., Takaya, H., Akutagawa, S., Sayo, N., and Saito, T. (1989). Stereoselective hydrogenation via dynamic kinetic resolution. J. Am. Chem. Soc. *111*, 9134–9135.

182. Maeda, T., Makino, K., Iwasaki, M., and Hamada, Y. (2010). Diastereo- and enantioselective hydrogenation of α-amino-β-keto ester hydrochlorides catalyzed by an iridium complex with MeO-BIPHEP and NaBArF: catalytic cycle and five-membered chelation mechanism of asymmetric hydrogenation. Chemistry *16*, 11954–11962.

183. Wu, J., Sun, X., and Ye, S. (2006). Unexpected highly efficient ring-opening of aziridines or epoxides with iodine promoted by thiophenol. Synlett 2489–2491.

184. The lower yield for **89** was associated with a problematic purification.

185. Mathews, W.B., Foss, C.A., Stoermer, D., Ravert, H.T., Dannals, R.F., Henke, B.R., and Pomper, M.G. (2005). Synthesis and biodistribution of ^{11}C-GW7845, a Positron-emitting agonist for peroxisome proliferator-activated receptor-γ. J. Nucl. Med. *46*, 1720–1726.

186. Lee, B.C., Dence, C.S., Zhou, H., Parent, E.E., Welch, M.J., and Katzenellenbogen, J.A. (2009). Fluorine-18 labeling and biodistribution studies on peroxisome proliferator-activated receptor-γ ligands: potential positron emission tomography imaging agents. Nucl. Med. Biol. *36*, 147–153.